CHALMERS
UNIVERSITY OF TECHNOLOGY

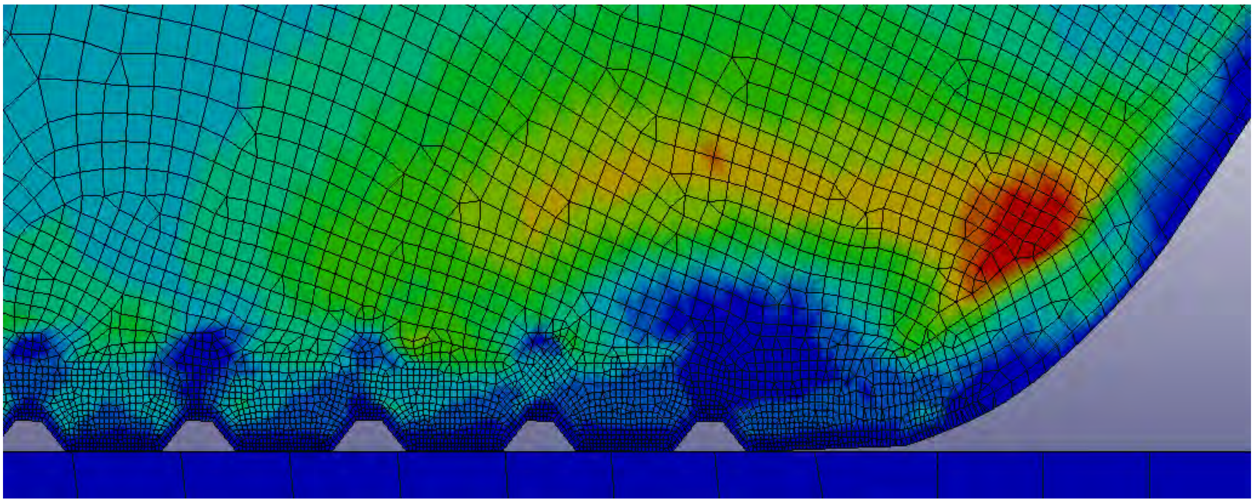

Wave propagation in human tissue from transient high frequency vibrations

Master's thesis in Biomedical Engineering

PRIYANKA MATHIYALAGAN
PARSIA NADAFAN

Department of Mechanics and Maritime Sciences
CHALMERS UNIVERSITY OF TECHNOLOGY
Gothenburg, Sweden 2020

MASTER'S THESIS IN BIOMEDICAL ENGINEERING

Wave propagation in human tissue from transient high frequency vibrations

PRIYANKA MATHIYALAGAN
PARSIA NADAFAN

CHALMERS
UNIVERSITY OF TECHNOLOGY

Department of Mechanics and Maritime Sciences
Division of Dynamics
Chalmers University of Technology
Gothenburg, Sweden 2020

Wave propagation in human tissue from transient high frequency vibrations
PRIYANKA MATHIYALAGAN
PARSIA NADAFAN

Supervisors: Håkan Johansson, Hans Lindell
Examiner: Viktor Berbyuk

Master's Thesis 2019:04
Department of Mechanics and Maritime Sciences
Division of Dynamics
Chalmers University of Technology
SE-412 96 Gothenburg
Telephone +46 31 772 1000

Cover: Wave propagation, Finite element model, Effective strain, Impact wrench

Printed by Chalmers digital tryck
Gothenburg, Sweden 2020

Wave propagation in human tissue from transient high frequency vibrations
PRIYANKA MATHIYALAGAN
PARSIA NADAFAN
Department of Mechanics and Maritime Sciences
Division of Dynamics
Chalmers University of Technology

Abstract

Hand-arm vibration injury from the daily exposure of vibrating hand-held machine is one of the common health injuries and causes severe nerve cell damage to the person operating the machine for a long time. The major health problems caused by daily use of vibrating tools causes signs and symptoms like peripheral vascular and peripheral neural disorders of the fingers and hands. These disorder symptoms include numbness, pain, and blanching of the fingers.

ISO 5349 claims that the vibrating machines with frequencies in the range of 8-1250 Hz must be regulated. However, vibrations with frequencies higher than 1250 Hz from machines like an impact wrench or dental drills can also damage nerve cells and blood vessels.
The objective of this thesis is to study wave propagation in human tissue from transient high frequency vibration of machines tools. The software LS-DYNA is used for performing the simulation and analyze the results. The 2D cross-section finite element model is created for the simulation to see the wave propagation into the finger tissue. The following analysis of simulation results shows that the different load cases from the hand-held vibrating machines affect the skin. However, the change in bulk modulus and decay constant does not make much difference. The intermediate skin layer has more impact caused by the hand-held vibrating machines.

Keywords: Hand-arm vibration, Impact wrench machine, Rammer, High-frequency vibration, Strain and strain rate, HAVS, FEM, ISO 5349

Preface

In this study, pull-through and push-in computational simulations have been done with LS-DYNA. This study is a part of a master thesis project concerning High-frequency vibration in hand-held machines. It was carried out at the Department of Mechanics and Maritime Sciences, Division of Dynamics, Chalmers University of Technology, in cooperation with RISE IVF AB, Sweden.

The thesis is supervised by Håkan Johansson, Hans Lindell, and the examiner of the thesis is Viktor Berbyuk. All tests have been carried out in the Chalmers computer at department of Mechanics and Maritime Sciences at the Chalmers University of Technology. We would also like to thank RISE IVF AB for their co-operation and involvement. Finally, it should be noted that the simulations could never have been conducted without the guidance of the professors and the supervisors.

Acknowledgements

We would first like to thank our thesis supervisors Hans Lindell from RISE IVF AB and Håkan Johansson at the Chalmers University of Technology. The door to Prof. Viktor Berbyuk's office was always open whenever we ran into a trouble spot or had a question about our research or report writing. We are consistently allowed this paper to be our work but steered us in the right the direction whenever he thought we needed it.

Finally, we must express our very profound gratitude to our parents and the faculties in the Chalmers University of Technology for providing us with unfailing support and continuous encouragement throughout our years of study and through the process of researching and writing this thesis. This accomplishment would not have been possible without them, thank you.

Priyanka Mathiyalagan
Parsia Nadafan

Contents

List of Figures

List of Tables

1 Introduction

This study is a master thesis project at Chalmers University of Technology at the Department of Mechanics and Maritime Sciences. The research is proposed by RISE Research Institutes of Sweden-RISE IVF AB in Mölndal to determine the extent to which the transient high-frequency vibrations propagate in human tissue in the finger. As a result, it can prevent the risk of daily exposure of people using the hand-held vibrating machines.

The current standard for risk evaluation takes no account of vibrations with a frequency content above 1250 Hz [1], which implies that the vibration from tools with a striking impact approach, such as Impact wrenches, is greatly underestimated as the vibration's primary energy content is far above 1 kHz.The transients often have an acceleration level exceeding 10,000m/s2.
.

1.1 Problem Definition and Project Goal

The FEM model for the finger needs to create based on the frequency ranges for the hand-held machines from the ISO 5349[2]. This study investigates the extent to which the transient high-frequency vibrations propagate into human tissue in the finger due to different load cases, material parameters, and the geometry in the fingerprint model. The results need to be analyzed based on the pressure, stress, principal strain, strain, and strain rate in the finger for high-frequency machines like Impact wrenches. and those results have to be compared with low-frequency tools like Rammer.

Sub Goals: The study aims at answering the following questions:

- To what extent will transient high-frequency vibration propagate into human tissue in the finger for different load cases, material parameters predicted.
- How do different load cases affect the pressure, stress, strain, and strain rate?
- How do changes in Bulk modulus and Decay constant effect the pressure, stress, strain, and strain rate?
- How does change in shear modulus affect the pressure, strain, and strain rate?

2 Theory

Daily exposure of using vibrating equipment with high frequency appears to be associated with neurological effects such as HAVS [3]. LS-Dyna software is used to perform simulations to obtain the desired results. However, the main desired results are based on obtaining strain and strain rate, but the pressure, stress, and other related factors were subsequently studied.

2.1 Skin layers

Human skin is the largest organ in the body, consisting of three layers, i.e., epidermis, dermis, and the subcutaneous fat.

The outermost layer of the skin is the Epidermis, responsible for the firmness and rigidity of the skin. The next layer is the dermis, divided into the papillary dermis and reticulum dermis [4].

The upper layer is the papillary dermis, and the lower layer is the reticular dermis, which contains blood vessels and nerves. The connective tissue existing in the dermis is essential properties that cause the skin elasticity, and also it is essential for collagen production. The subcutaneous fat is comprised of the third layer of the skin.

The subcutaneous layer at the bottom is connected to the skin's dermis, which is vital in protecting the body against mechanical trauma. The Epidermis consists of four to five-layer depending on the type of the skin.

Thick skin has five layers, and it is found in the palms of the hands and on the soles of the feet. Thin skin has four layers that cover most of the body. The skin model has all five layers. The bottom or deep layer is called the stratum basale, and the next layer is the stratum granulosum. This layer is comprised of three to five layers of keratinocytes. The next layer is a stratum lucidum that is a thin layer of dead cells in the Epidermis that cover the outside of the body, which is found in the palms and soles of the feet [5].

2.2 Software LS-Dyna

LSTC (Livermore software technology corporation) develops the LS-DYNA software. It is a general-purpose finite element program used for simulating complex real-world problems. This software is used in automobile, aerospace, military, manufacturing, and bio-engineering industries. LS-DYNA supports Unix, Linux, and Windows-based computers, platforms[6]. LSTC also develops its pre-processor, LS-PrePost, which is freely distributed and runs with¬out a license.

LS-Pre post: The LS-Prepost is advanced software that contains both pre and post-processor that can come along with LS-DYNA software packages. The software's user interface is designed to be both efficient and easily understandable. The Preprocessor is used to define the inputs such as Mesh, geometry, and material parameters, similarly, the post-processing is used to obtain the output results. LS-PrePost can run in all types of computer operating systems.

2.3 Strain and strain rate

The strain is defined as the response of a system when there is a stress applied in the system. When the external force is applied to the material, it produces stress, resulting in the material being deformed. Strains may be divided into regular strains and shear strains based on the forces that cause the deformation. A strain which is caused by forces that are perpendicular to the planes or cross-sectional areas of the material, such as volume that is under pressure on all sides.

Strain rate is the speed or velocity at which the deformation of an object from its original shape occurs. Depending on the way the applied force or stress deformation can occur in any direction. Strain rate varies for different materials, and it changes at different temperatures and applied pressures.

2.4 High frequency and neurological effects

The International Standards Organization (ISO) regulates the daily exposure limits to the vibrations from these tools. The regulation, ISO 5349, is under the topic of Mechanical Vibration, which is used to the measurement and also for analyzing the human's daily exposure of hand-transmitted vibration at the industries. It is based on a subjective assessment that averages out the frequency and states that the vibration with the frequency range 8-1250 Hz are dangers and frequencies higher than 1250Hz are not. The suggestion that high-frequency vibration is not causing damage is contradictory to the fact that neural symptoms have been found among dentists (as one example), using high-speed drills (with high vibration frequencies) as part of their daily work [7], which supports the imminent need for a more effective and accurate method for estimating risk when handling high-frequency tools.

Working regularly with a hand-held or hand-guided power tools such as road breakers, jigsaws, and chainsaws, hammer drills, hand-held portable grinders, floor polishers, nut runners for more than a few hours, each day can lead to shaking in the arms and even possibly other parts of the body that is known as hand-arm vibration. Nowadays, what is known as hand-arm vibration syndrome or HAVS is the effects of excessive prolonged exposure to hand transmitted vibration. Hand-arm vibration syndrome (HAVS), as mentioned, is caused by occupational exposure to vibrating hand tools near fingerprint where nerves are present. It has three components such as vascular, in the form of secondary Raynaud phenomenon, sensorineural and musculoskeletal [8].

A cause-effect relation carpal tunnel syndrome (CTS) and exposures to vibrating hand-held tools seem probable [9]. Hand-arm vibration syndrome affect to varying degrees the blood vessel the nervous system, changes in muscles, tendons, and joints of the hand's wrists and arms.

The symptoms and effects of HAVS most commonly result in having pins and needles (tingling), burning, or itching, loss of grip strength, loss of feeling (numbness) in the hand's palm and the fingers, especially the thumb and index finger [10].

Stop working with vibrating tools that may prevent mild symptoms from worsening, such as tingling or non-sensation, which disappears after a short while. However, hand and arms shaking, numbness, or tingling sensation is still felt after using a power tool for a long time. In severe cases, a permanent numbness may extend along with affected fingers, and people may experience worse attack especially in colder weather that could last an hour.

These attacks also become painful for the person who may also experience a loss of usability dexterity or strength in their hand, becoming unpleasant as it weakens the ability to grip objects. A tingling, numbness or shaky feeling in hands or fingers loss of color in the hands followed by a red rush painful attacks that leave the hands weak, are essential signs of HAVS syndromes.

The study should be considered an influential contribution to knowledge about an exposure relationship between neurological symptoms and HAVS exposure to which be at an interface between soft tissue.

2.5 Finite element method

Finite element modeling is becoming increasingly popular. The finite element method or FEM is a numerical technique for solving engineering problems and performing computer-aided engineering analysis. The 2D cross-section finger model, which represents three skin layers, include the finger tissue, Epidermis, and stratum corneum. To determine shear modulus of skin layers, they will be adjusted in the FE-model until identical results are generated. The computational FE model of the finger was constructed in experimental work by a Pressure-device used to give consistent pressure on the top of the finger which shaped a fingerprint on a mold that was located under fingers.

The FE model would be the fingerprint geometry was made later by scanning this mold. The possible existing gap in finger geometry was filled computationally. The shape of the FE-model was created with the help of the parametrization of the fingerprint in Matlab.

Research related to study the impact of vibrating tools on soft tissue was performed mainly in the palm and finger of the hand that has direct contact with vibrating tools and also in the brain of tissue that was considered to apply an axial load at different rates. The output result, such as the resulting displacement and a mathematical model for energy function, was obtained by using an attached micrometer. Due to experimental study constrains, the obtaining results related to parameters analysis are limited.

In recent studies, a fingertip was subjected to cyclic loading at different frequencies for a computational analysis by using an FE model of the finger. The exposure-response relationship was analyzed by considering a threshold that led to the conclusion that exposure on Temporal Threshold Shift (TTS) is associated with the dynamic distribution of strain. Furthermore, aiming at evaluating the effect of shear and compression in the finger few simulations were performed using Finite Element Analysis (FEA) to assess 3D shear waves of different incident angles.

3 Computational Methodology

3.1 Simulation process

The simulations are performed based on the load cases, geometry and the material parameters to analyze the maximum strain and the strain rate in each layer of the skin. The simulation is done in LS-DYNA. The simulation can show how the shear modulus in the different layers get affected and understand what happens to the nerve cells in the finger. Here, the Geo-intermediate fingerprint model (Subsystem) is used as a subsystem to perform throughout the primary simulation process. The estimated simulation time is 4 hours.

3.2 Simulation setup (Input Data)

Pre-processing is used for defining Input data in LS-DYNA, such as load cases, material parameters, and the geometry, which is used for processing the output results from the LS-DYNA analysis. The input data are saved in the form of Keyword (.k file) in LS-Dyna.

3.3 Mesh

A mesh is defined as a network that is made up of cells and points. Mesh is used in the finite element model to define the object's geometry or vertices (See fig.1).

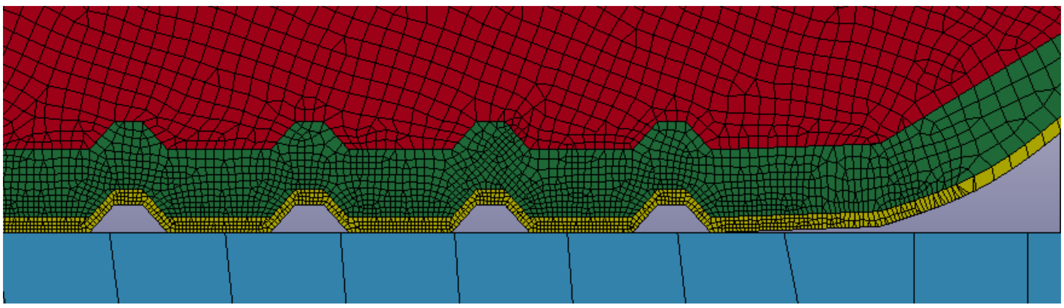

Figure 1: Mesh.

3.4 Boundary conditions

Boundary conditions are used to set the vectors and its coordinate system and also define the load curve. For determining values in LS-Dyna *BOUNDARY PRESCRIBED MOTION SET* option is used[11] (See.fig.2).

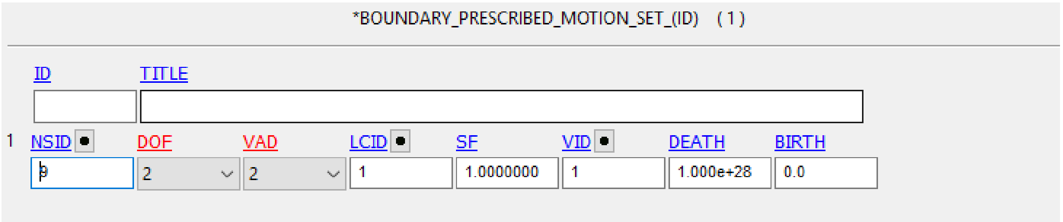

Figure 2: Boundary Conditions.

- DOF defines the direction on of load, global or local direction on
- VAD (Velocity, acceleration/Displacement)defines the load type
- LCID (Load curve ID) defines the variation in time for the applied load cases
- SF (Scale amplitude) of the load curve
- VID (Vector ID) for vector to be used if DOF=4 or 8
- DEATH/BIRTH defines the boundary condition active range of time

3.5 Defining curve and vector

This section describes the method for loading the curves and vector as an input in the keyword manager under the section for defining the load curve and load vector for the simulation in LS-Dyna[11] (See fig.3 and fig 4).

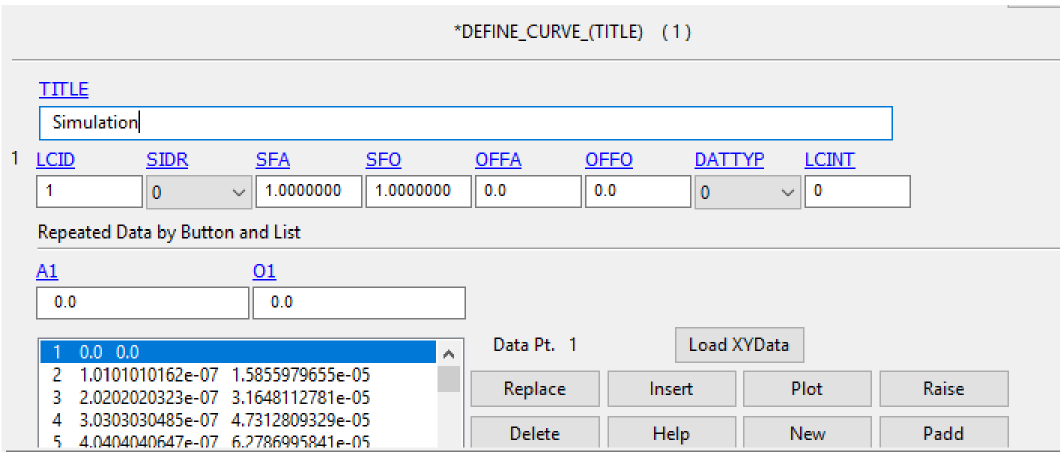

Figure 3: Load Curve.

- LCID defines Load curve ID.
- SIDR defines Stress initialization by dynamic relaxation

- SFA defines Scale factor for X axis
- SFO defines Scale factor for Y axis
- OFFA defines Offset for X axis
- OFFO defines Offset for Y axis
- DATTYP defines Data type

The vector is defined by defining the coordinates of the system

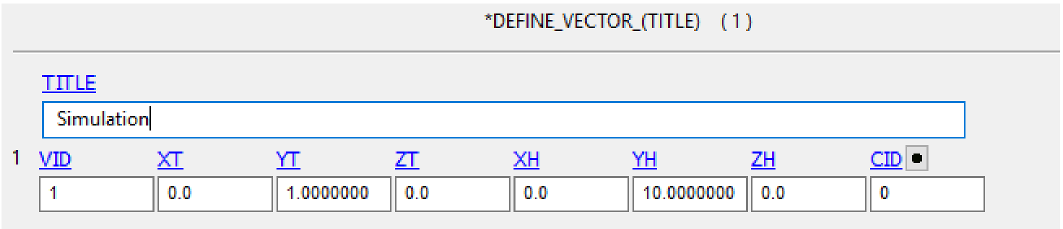

Figure 4: Load Vector.

- VID defines Vector ID
- XT defines X-coordinate of tail of vector
- YT defines Y-coordinate of tail of vector
- ZT defines Z-coordinate of tail of vector
- XH defines X-coordinate of head of vector
- YH defines Y-coordinate of head of vector
- ZH defines Z-coordinate of head of vector
- CID defines Coordinate system ID to define vector in local coordinate system.

3.6 Part selection

FEM fingerprint model has four parts, represents the skin layers and the tool, which can be seen in figure 5. The Yellow layer represents as Epidermis (thin layer), the outermost layer of the skin, the Green layer represents Dermis (Intermediate layer), the red layer represents Soft tissue (thick layer), and the blue layer represents the tool,(See fig.5 and fig 6).

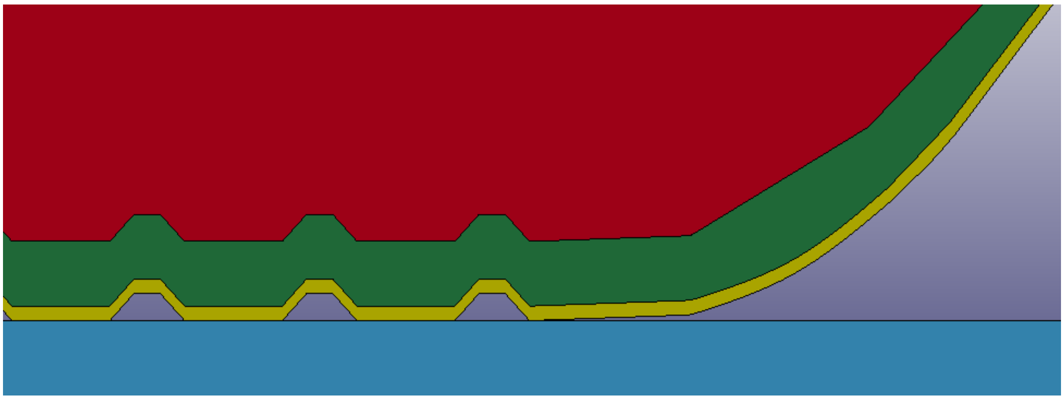

Figure 5: Defining Parts in FEM.

The part can be selected in the keyword manager in LS-Dyna under the PART section; part ID, element ID, material ID can be defined[6] (See fig.6).

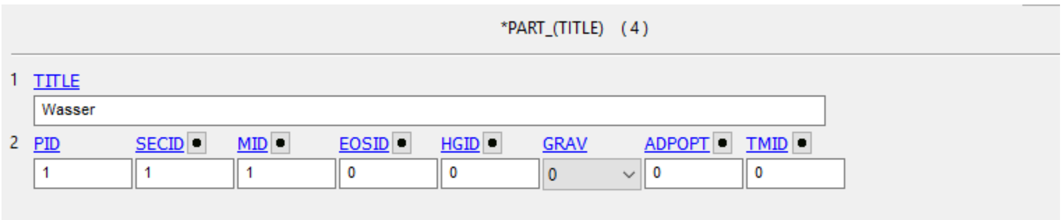

Figure 6: Part Selection in LS-Dyna.

3.7 Element selection

Elements can be selected based on the high strain and strain rate in the different skin layers. The following elements are selected in each layer of the finger, and also the symmetry line is considered for selecting the elements which are used for the study[11]. The following elements are (Element A- 346208, Element B- 372361, Element C - 88046), (See fig.7)

Figure 7: Selected elements.

Here the finger model can be seen with the elements selected on it. The elements are selected in all the three skin layers of the finger in order to see where the maximum strain and strain rate are occurring. By this strain and strain rate data is collected for this study. For measuring strain and strain rate, the "Mean IPT effective strain and "Effective strain (v-m) strain rate are selected in the LS-DYNA.

3.8 Applied load cases

Once the FEM model is created, the required load pules are applied to the model using LS- DYNA. The existing load cases given from RISE IVF AB are taken as a reference for creating new load pulses used in this study. In this study, the three load cases applied to the models based on displacement in millimeters peak to peak and provided by RISE IVF AB. The load cases are defined in the X-Y plane as in the form of sinusoidal acceleration. The obtained curves from the load cases have different amplitude and the same frequencies (T=Time period). Once the load case is created, then it is inserted in the LS-DYNA to plot the graph, (See fig.8)

Load case 1: Displacement(mm,peak) = 0.0025,$|a_{max}| = 10,000m/s^2, T = 0.0001s$

Load case 2: Displacement(mm,peak) = 0.00025, $|a_{max}| = 100,000m/s^2, T = 0.00001s$

Load case 3: Displacement(mm,peak) = 5.6290,$|a_{max}| = 50m/s^2, T = 0.066s$

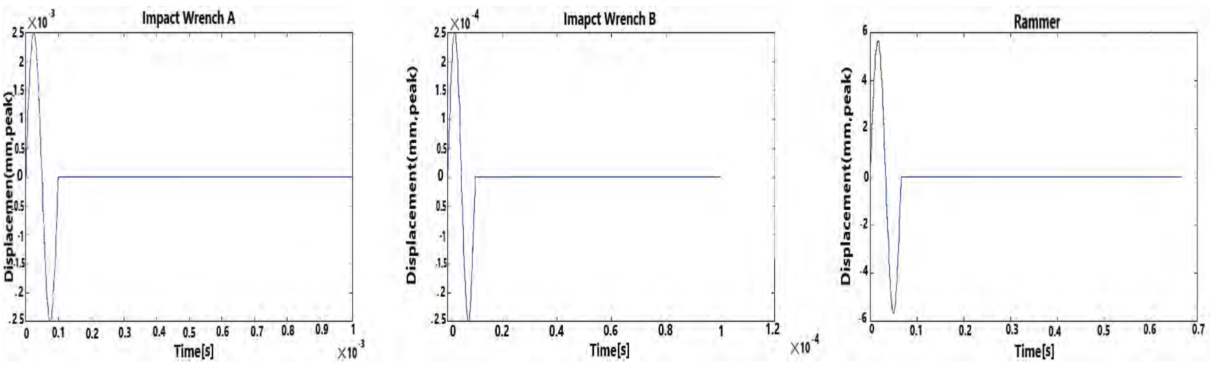

Figure 8: Load cases used for simulations.

3.9 Material parameters

Material parameters may differ for each person based on age and environmental factors. The epidermal layers start to become thin for various reasons: aging of persons, less moisture content in the skin, and daily exposure of using vibrating machines. The material has different characteristics behavior such as elastic and viscoelastic. Viscoelastic material property has the characteristics of both viscous and elastic when it is subjecting to deformation. This material withstands the shear flow and strains linearly concerning the time while the external stress is applied to the object, the strain of the elastic material gets stretched, and when the external stress is removed, it returns to their original shape. Viscoelastic materials have elements of both the material properties, and they exhibit time-dependent strain[3]. The material parameters for the different skin layers are listed below (table 1 and table

2). Shear modulus is described as the ratio of shear stress to the shear strain[12]. It is denoted by G_0 and G_∞ represents short-time shear modulus to a long-time shear modulus[13]. The unit of shear modulus is [MPa].

$$G(t) = G_\infty + (G_0 - G_\infty)e^{-\beta t} \tag{1}$$

The shear modulus is defined to measure the ability of a material in order to resist transverse deformations. It is an index of elastic behavior only for small deformations, after which the material can return to its original shape. Large shearing forces can cause permanent deformation. The shear modulus is also called as the rigidity. From Table 2, it can be seen that shear modulus is varied for all the skin layers. Still, Bulk modulus and Decay constant are kept constant all over the simulation, The changing in Bulk modulus, and beta does not show much difference, which is why keeping those values constant for the simulations.

Skin layers	Shear modulus[MPa]	Bulk modulus[MPa]	Decay constant $\beta[S^{-1}]$
Soft tissue	0.0017 0.017	2190	215
Epidermis	0.021 0.2	2190	215
Stratum Corneum	0.6 10	2190	215

Table 1: Material parameters used in simulations.

Epi G0[Mpa]	Epi GI[Mpa]	St.cor G0 [Mpa]	St.cor GI[Mpa]	Mat G0[Mpa]	Mat GI[Mpa]
0,021	0,0200004	0,6	0,58068	0,0017	0,0005732
0,021	0,0200004	0,6	0,58068	0,017	0,005732
0,021	0,0200004	10	9,678	0,0017	0,0005732
0,021	0,0200004	10	9,678	0,017	0,005732
0,2	0,19048	0,6	0,58068	0,0017	0,0005732
0,2	0,19048	0,6	0,58068	0,017	0,005732
0,2	0,19048	10	9,678	0,0017	0,0005732
0,2	0,19048	10	9,678	0,017	0,005732

Table 2: Shear modulus parameters used in simulations.

3.10 Geometry

The geometry is defined based on the thickness of the skin layers in the finger; these geometries can be varied based on the individual persons. To analyze the strain and strain rate, varying layers of finger skin, apply separate load cases. The experiment is performed in LS-DYNA to obtain the strain and strain rate for each skin layer. The following geometry for the stratum corneum and the epidermis is given below, and the soft tissue is kept constant (See Table 3).

Geometry type	Tissue layer	Thickness [µm]	Area [mm2]
Thin skin	Epidermis	80	5.06455
	Stratum corneum	25	1.39954
Intermediate Skin	Epidermis	145	5.81096
	Stratum Corneum	32.5	1.48592
Thick Skin	Epidermis	210	6.55406
	Stratum Corneum	40	1.57438

Table 3: Geometry.

3.11 Decay constant and Bulk modulus

The unit forDecay constant is β [s^{-1}]. Different beta values are listed in Table 4. These values are used in all the simulations to analyze whether changing beta values makes it more different. The results can be explained in the upcoming sections.

Bulk modulus is a numerical constant that describes material behavior such as stress or strain and the elastic properties of a solid or fluid when the surface is under pressure. The unit for Bulk modulus is [MPa]. Different Bulk modulus values are listed below in Table.4. These values are used to analyze the variation in Bulk modulus and decay constant for different load cases.

S.no	Decay constant $\beta[s^{-1}]$	Bulk modulus
1	2.15	1095
2	21.5	1971
3	215	2190
4	2150	2409
5	21500	3285

Table 4: Decay constant.

4 Data analysis and its results

This chapter considers data analysis and displays the obtained results in the form of graphical representations and measures the strain and strain rate pressure, stress, and the principal strain. The pressure is calculated for each chosen element in different skin layers to see the viscoelastic material behavior for various load cases. Simulation results show that the high-frequency displacement from the impact tools creates a wave that propagates into the tissue. Impact wrench A and Impact wrench B used the same material parameters for all the simulations. The same material parameters like Impact wrenches are not suitable for Rammer. So, machine Rammer has a different Bulk modulus, which is 21.9 MPa, is changed to fix the movement between the fingerprint and the tool.

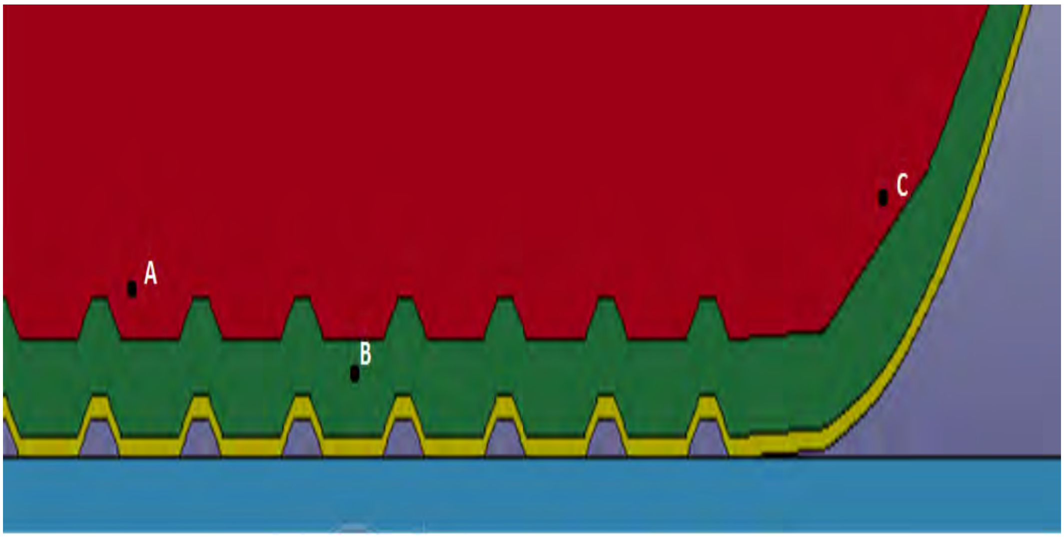

Figure 9: Selected elements

4.1 Pressure

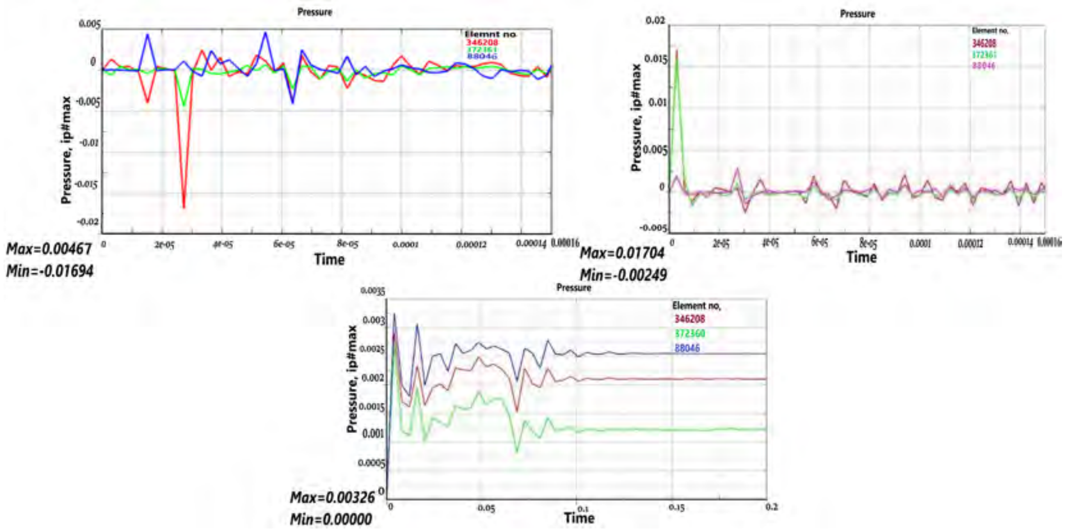

Figure 10: Pressure comparison for 10,000 Hz , 100,000 Hz and 15 Hz respectively.

Time-frequency analysis of pressure yields a pressure fluctuation pattern, which occurs in the impact duration of finger model loading on the solid contact surface. Impact wrench B with 100,000 Hz frequency obtains its maximum pressure in its first cycle with 0.01704, which is more than the other Impact wrench. The initial impulsive pressure in Impact wrench B, near to element-A and element-B visibly occur in the very first cycle, which sharply dropped down as the simulation run further. Taking a closer look at the Impact wrench B, element-A near to symmetric line has the maximum pressure of 0.01704 and the minimum pressure, which is -0.00249.

Same as Impact wrench B, near to element-A, Impact wrench A with 10,000 Hz frequency, has a sharp pressure peak, more precisely a downward-facing peak, in the second cycle. In the first cycle, pressure variation is not such prominent as it is in the second cycle with minimum pressure, i.e., -0.01691.

Consequently, this machine has no such high maximum pressure as others. The overall Pressure comparison for Impact wrench A, Impact wrench B, and Rammer yields that this machine, i.e., Impact wrench B, has the most maximum pressure compare with other hand-held tools, i.e., Impact wrench A and Rammer. In summary, the obtained results indicate that after a sudden peak of pressure, i.e., a large increase-decrease of the pressure peak in the impact duration, the pattern transforms into a steady-state pressure fluctuation form.

4.2 Stress

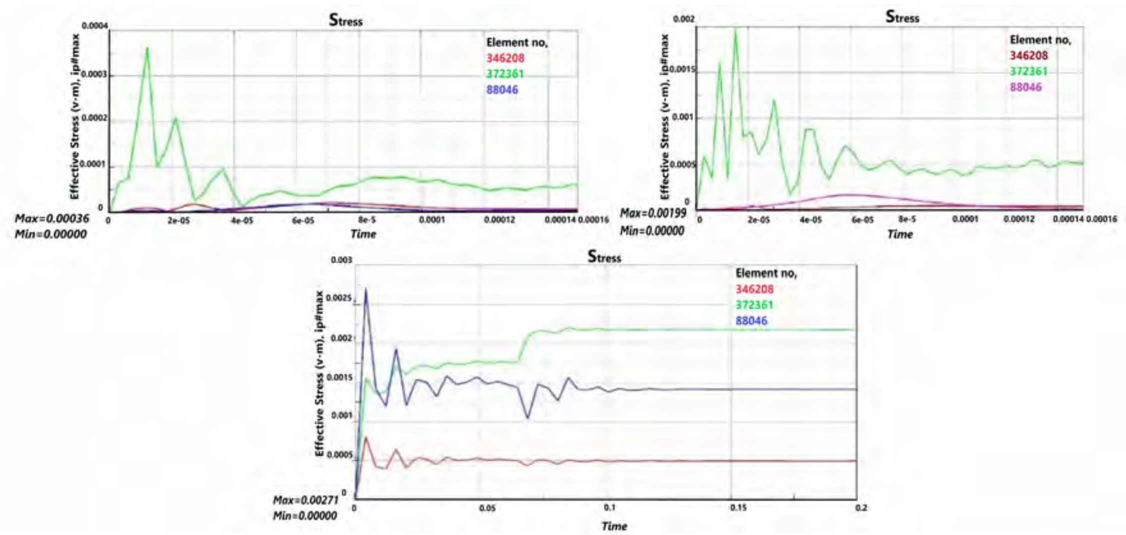

Figure 11: Stress comparison for 10,000 Hz , 100,000 Hz and 15 Hz. respectively

Maximum effective stress for both Impacts wrenches A and B occurs in the first time cycle, i.e., 0.00036 and 0.00199. As shown in figure 11, element B in the middle layer has maximum stress variation than other elements, i.e., element A and element C; hence, apart from a few particular times, stress distribution in these elements is close to zero.
Conversely, the overall stress distributions of Rammer over time are slightly higher. Accordingly, the stress comparison for Impact wrench A and Impact wrench B and the Rammer suggests that the Rammer has maximum effective stress that is 0.00271. Like Impact wrenches, the minimum effective stress is zero.

4.3 Upper max Principal Strain

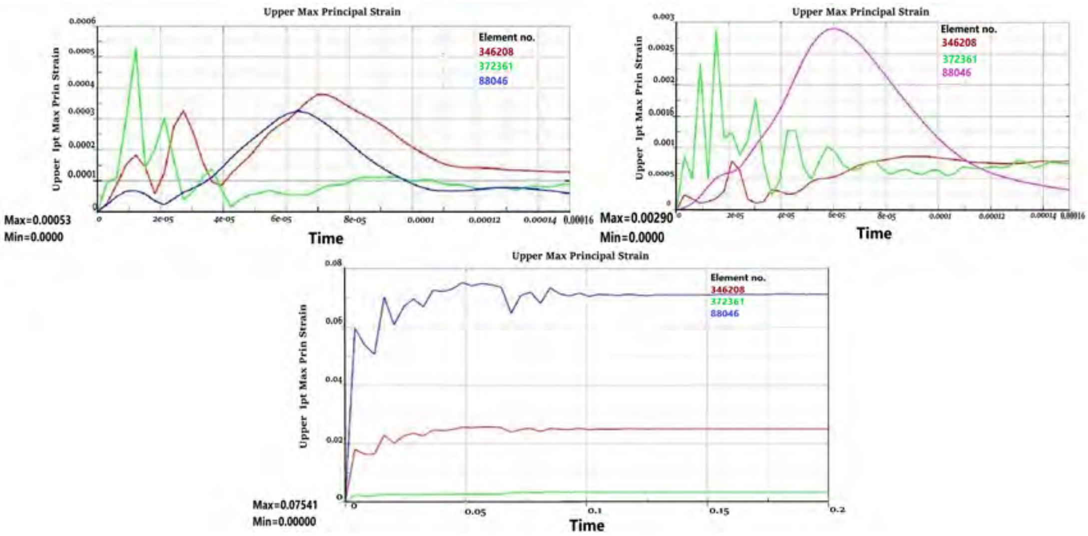

Figure 12: Principal Strain comparison for 10,000 Hz, 100.000 Hz and 15 Hz respectively

The maximum principal strain for the Impact wrenches A and B are 0.00053 and 0.00290, respectively. Principal Strain's comparison for Impact wrench A and Impact wrench B and the Rammer shows that the Rammer has a maximum principal strain of 0.07541.

4.4 Strain

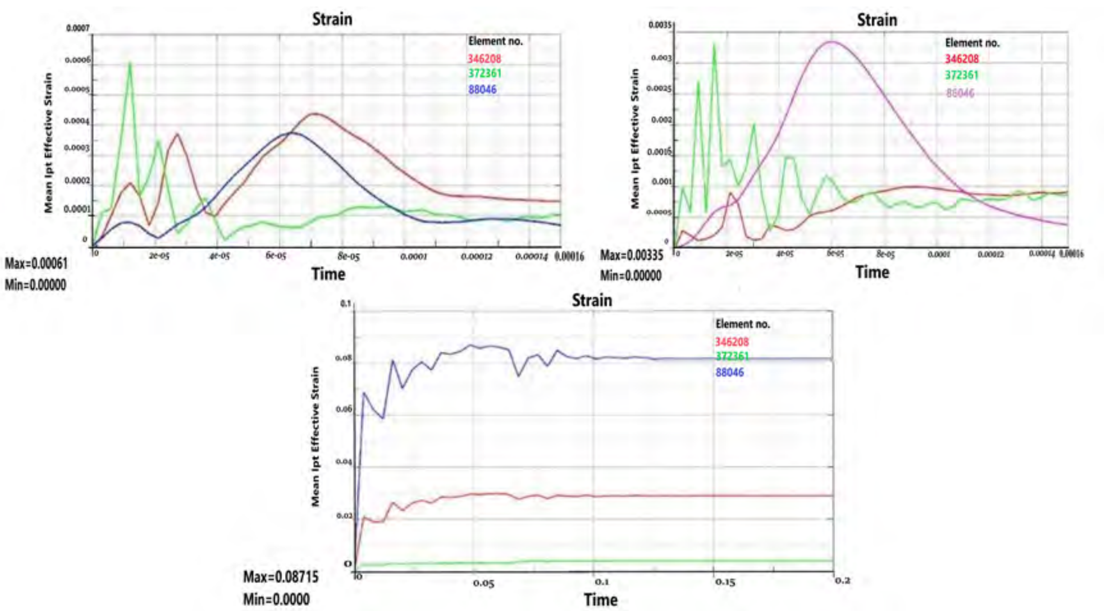

Figure 13: Strain comparison for 10,000 Hz , 100,000 Hz and 15 Hz respectively

The maximum effective strains for the Impact wrenches A and B are 0.00061 and 0.00335. The effective strain for Impact wrench B is higher than the Impact wrench A. Like previous results, Rammer has the maximum strain that is 0.08715 as compared to both the Impact wrenches A and B.

4.5 Strain Rate

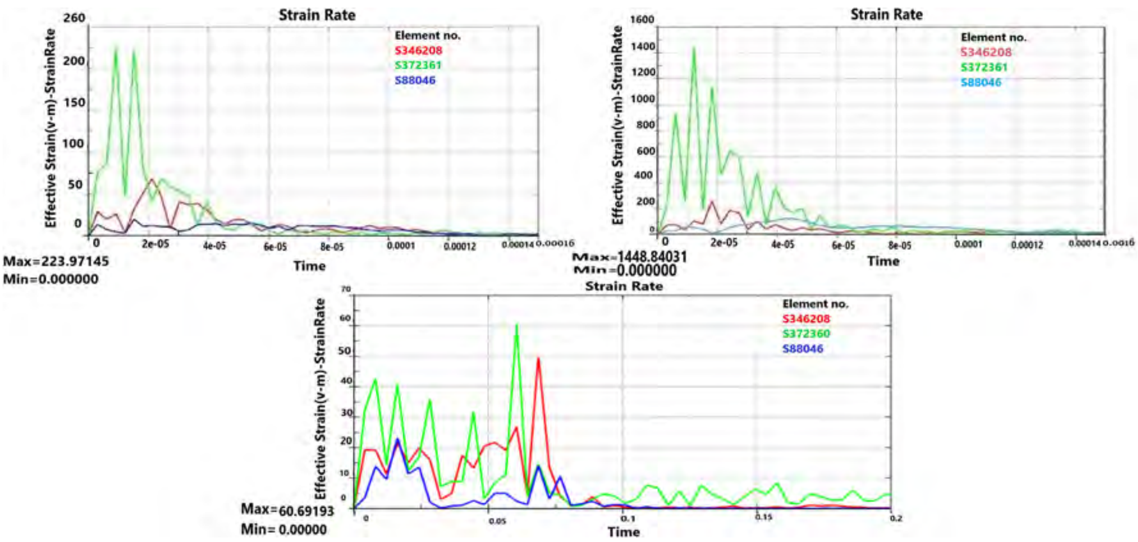

Figure 14: Strain Rate comparison for 10,000 Hz, 100,000 Hz and 15 Hz

The principal strain rate fluctuation occurs in the first cycle for both Impact wrenches A and B with 10,000 Hz and 100,000 Hz, i.e., 223.97 and 1448.8, respectively, but the minimum Strain rate is the same that is zero for each one. The significant strain rate for Rammer occurs in the second cycle in element B, which is 60.691.

5 Discussion

This study compares various vibrating hand-held machines to analyze pressure, strain, and strain rate distribution in the skin layer. While running the simulation, the fingerprint model and the tool's initial movement needs to be decreased, which ultimately achieved by adding gravity to each fingerprint model with different load cases based on the acceleration for the first two load cases (Impact wrench A and Impact wrench B).

Still, in the case of load case 3 (Rammer), the given gravity is not sufficient for the finger model, which not resulting in the desired elimination of movement between the finger model and rigid surface. Figure 15 shows how the model responds the given gravity.

Consequently, the model Rammer with 15 Hz frequency applied another Bulk modulus value, i.e., 21.9 MPa, and gravity, 9.8 ms, was given to the model based on acceleration to fix the movement hence the results for Impact wrench A with 10,000 Hz frequency and Impact wrench B with 100,000 Hz frequency are established on entirely identical conditions, which is not the same for Rammer.

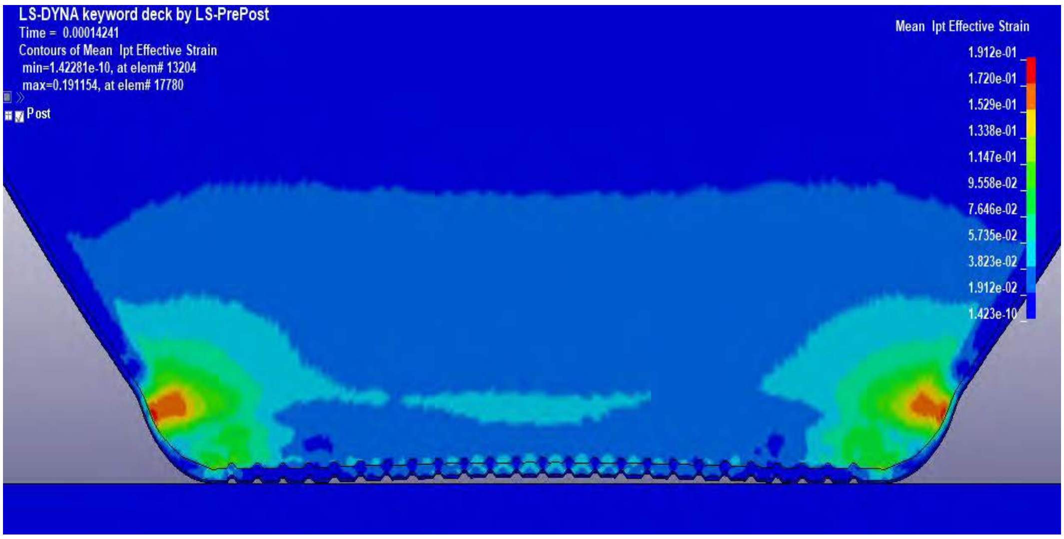

Figure 15: Rammer Simulation distribution

6 Conclusion

Running various simulations aiming to determine how frequency differences, i.e., low, high, and very high levels in the vibrating tool, could influence factors that result in neural disorders such as HAVS, comes the Rammer out with the highest impact. The obtained results are based on a change in its Bulk modulus, purposing reduction in the present movement between the fingerprint model and the tool. Except for pressure and strain rate, the obtained results imply that Rammer with 15 Hz has the highest strain, principal strain, and stress.

Impact wrenches Decay constant, and Bulk modulus for all simulations are constant, i.e., 215 s^{-1}, and 219 MPa, respectively. The variation result of the Decay constant, shear modulus and Bulk modulus are attached in the appendix. Impact wrenches comparisons yield that the Impact wrench B with 100,000 Hz has a higher pressure, strain, strain rate, principal strain, and stress than Impact wrench A with 10,000 Hz, and to the same extent, it has a higher risk for the users.

6.1 Outlook for future research

The suggestion for future work is to investigate the nerve cell damages, which is due to daily exposure to using hand-held machines for a long time. So, this can be useful to study the probability impact of these factors in Hand-arm vibration syndrome (HAVS).

Furthermore, since the ran simulations not performed with the same material parameters, the received results can not be a proper criterion for comparing these machines. Hence it would be desirable as future work to obtain reliable results based on identical conditions as well as running some simulations with different angles to study its possible effect on the strain and strain rate.

7 Bibliography

[1] James P, Galloway R. Arteriography of the hand in men exposed to vibration. In: Talor W, Pelmear P, editors. Vibration white finger in industry, vol. 4. London: Academic Press; 1975. 31–41.

[2] ISO 5349-2:2001(en) Mechanical vibration Measurement and evaluation of human exposure to hand-transmitted vibration. Available from: `https://www.iso.org/obp/ui/#iso:std:iso:5349:-2:ed-1:v1:en`

[3] Can Fam Physician. Hand-arm vibration syndrome What family physicians should know. Published: 2017 Mar; 63(3): 206–210. Available from:https://www.NCBI.nlm.nih.gov/pmc/articles/PMC5349719/

[4] Hani Yousef1; Mandy Alhajj2; Sandeep Sharma.Anatomy, Skin (Integument), Epidermis. Last Update: June 12, 2019.Avilable from:https://www.ncbi.nlm.nih.gov/books/NBK470464/

[5] Anatomy and Physiology, Chapter 5. The Integumentary System, Layers of the Skin.Available from:https://opentextbc.ca/anatomyandphysiology/chapter/5-1-layers-of-the-skin/

[6]LS-Dyna Available from: Urlhttps://builders.intel.com/datacenter/membership/lstc
[7] Rakesh Chowdhry, Vikas Sethi. Hand-arm vibration syndrome in dentistry: A review. Received Aug 11 2017, Revised Nov 3 2017, Accepted Nov 10 2017, Available online Nov 13 2017. Available from:
https://www.
sciencedirect.com/science/article/abs/pii/S2352081717301411

[8] Javid Hussain Sagar, Soniya T Lohana. Hand-arm Vibration Syndrome in Farmers and its Correlation with Degenerative Triangular Fibrocartilage Complex Injury. May 1, 2019.Available from:https://europepmc.org/article/PMC/6783529

[9] Falkiner S. Diagnosis and treatment of hand-arm vibration syndrome and its relationship to carpal tunnel syndrome.2003 Jul.Available from:https://www.ncbi.nlm.nih.gov/pubmed/12901208

[10] Canadian Centre for Occupational Health and Safety. Vibration - Health Effects.Date modified: 2020-01-15.Avilable from:https://www.ccohs.ca/oshanswers/phys$_agents/vibration/vibration_effects.html$

[11] LS-Dyna support-Mannuals Pre-processing and post-processing.Available from:`http://ftp.lstc.com/anonymous/outgoing/jday/manuals/LS-DYNA_manual_Vol_I_R6.0.0.pdf`

[12] ThoughtCo.Shear modulus definition. Available from:https://www.thoughtco.com/shear-modulus-4176406

[13] HANS LINDELL.Attenuation of hand-held machine vibrations.Published: Sweden 2017. Avilable from:http://publications.lib.chalmers.se/records/fulltext/253449/253449.pdf

[14] National Institute for Occupational Safety Health, Morgantown, WV 26505, USA. jwu@cdc.gov.Finite element analysis of the penetrations of shear and normal vibrations into the soft tissues at a fingertip.Published:2007 Jul;29(6):718-27. Epub 2006 Sep 7. Available from:https://www.ncbi.nlm.nih.gov/pubmed/16962362

[15] Sorbothane innovation products and vibration solution-The Difference Between Elastic Materials and Viscoelastic Materials. Available from:https://www.sorbothane.com/the-difference-between-elastic-materials-and-viscoelastic-materials.aspx

[16]Analysis of the point mechanical impedance of finger in vibration.Available from:https://www.ncbi.nlm.nih.gov/pubmed/16426886

[17] AZForumla.com. Avilable from:https://azformula.com/section/physics/elasticity/

8 Appendix Variation of simulation results

In this section, the variation of shear modulus, Bulk modulus, and Decay constant results are shown below. These results are analyzed to show that changing material parameters can affect the fem model or not.

8.1 Decay constant

Different Beta values such as 2.15, 21.5, 2150, and 21500 are used in the simulations to analyze whether the change in Decay constant may produce the strain and strain rate variation. After running various simulations, it clearly explains that change does not make much difference in the results.

Decay constant for load case 1 - 10,000Hz

Pressure

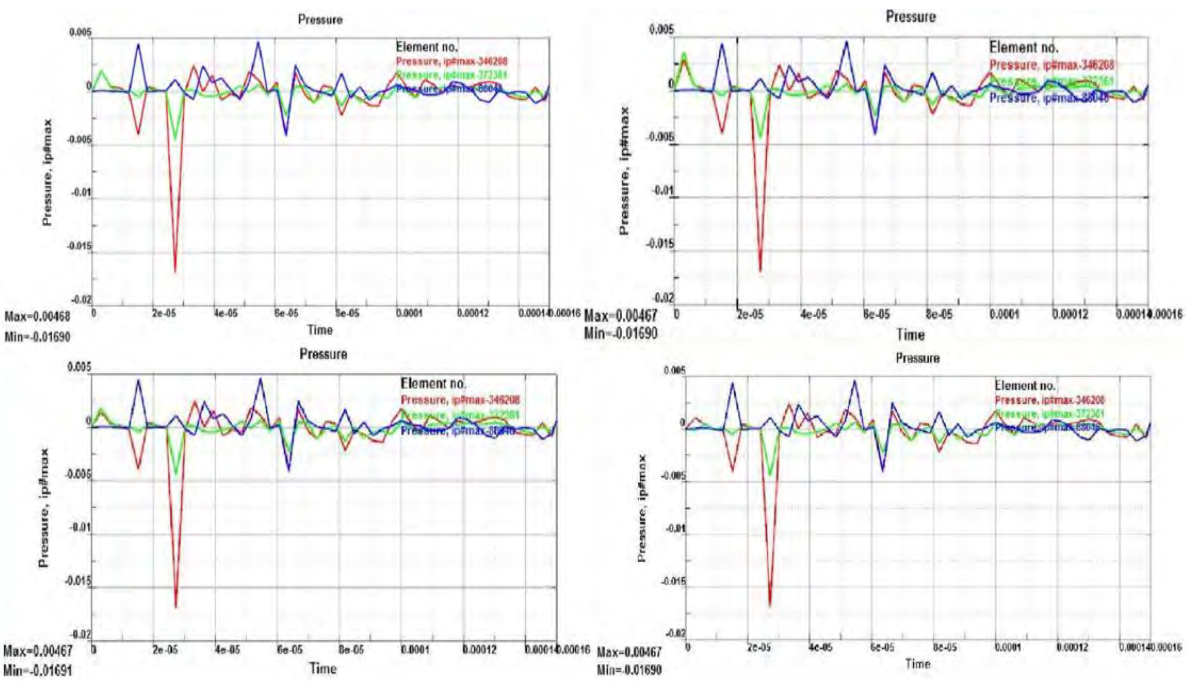

Figure 16: Pressure comparison for Beta load case 1 - 10,000Hz

Stress

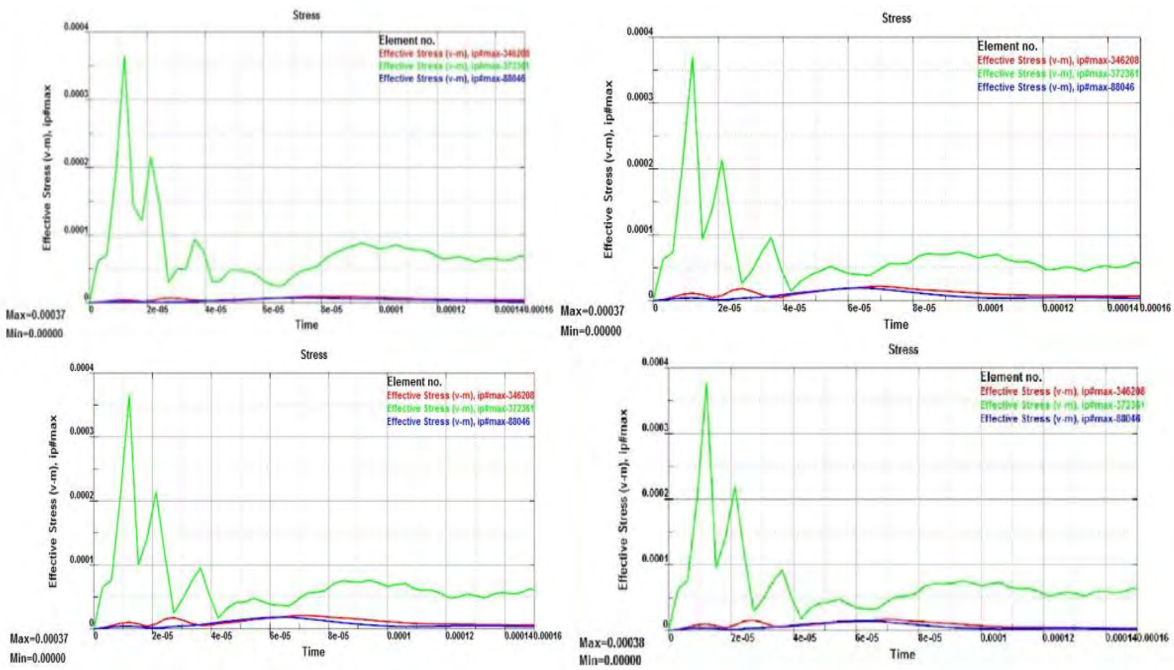

Figure 17: Stress comparison for Beta load case 1 - 10,000Hz .

Upper max Principal Strain

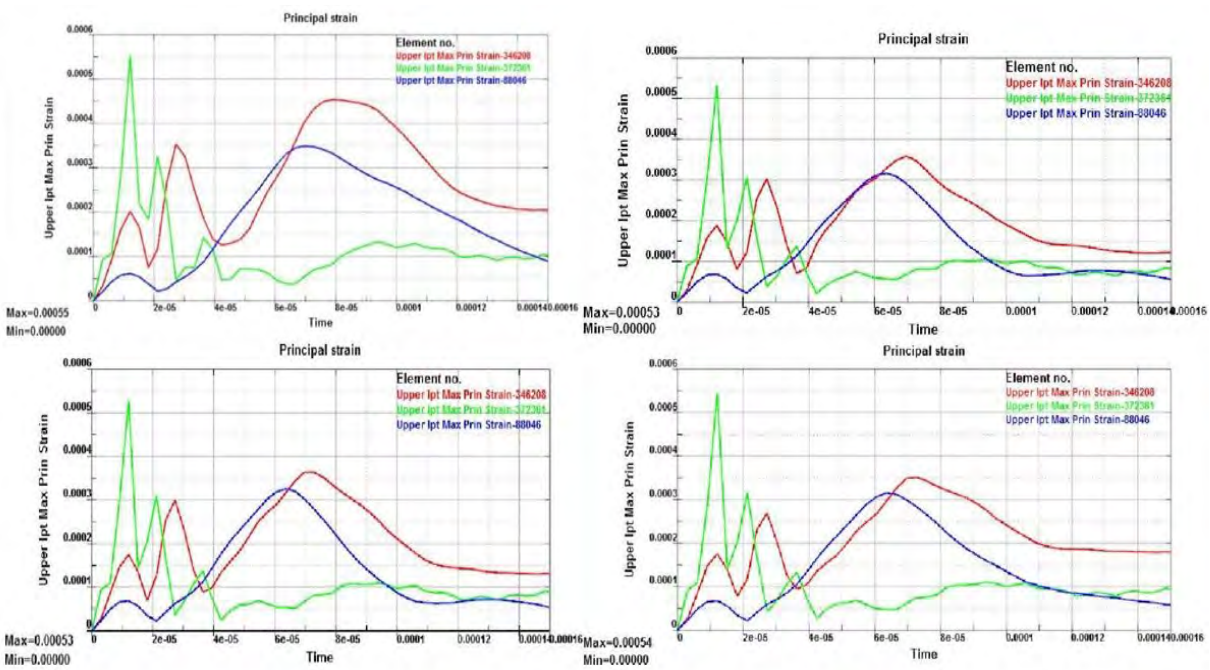

Figure 18: Upper max Principal Strain comparison for Beta load case 1 - 10,000Hz
.

Strain

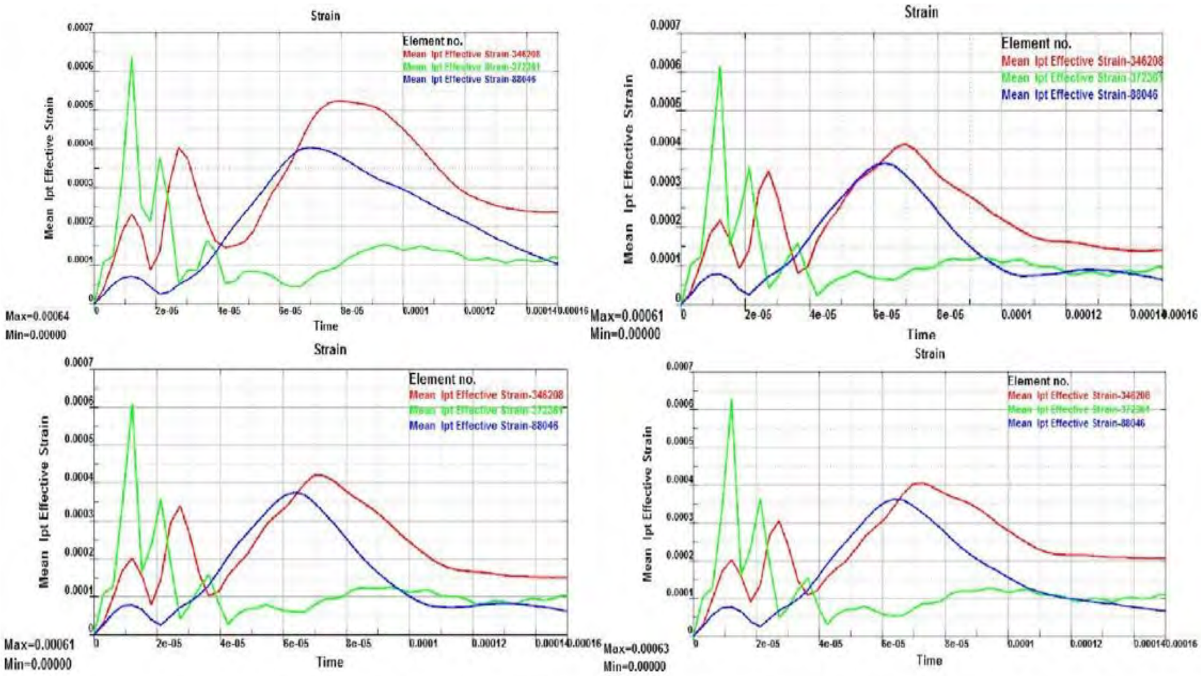

Figure 19: Strain comparison for Beta load case 1 - 10,000Hz .

Strain Rate

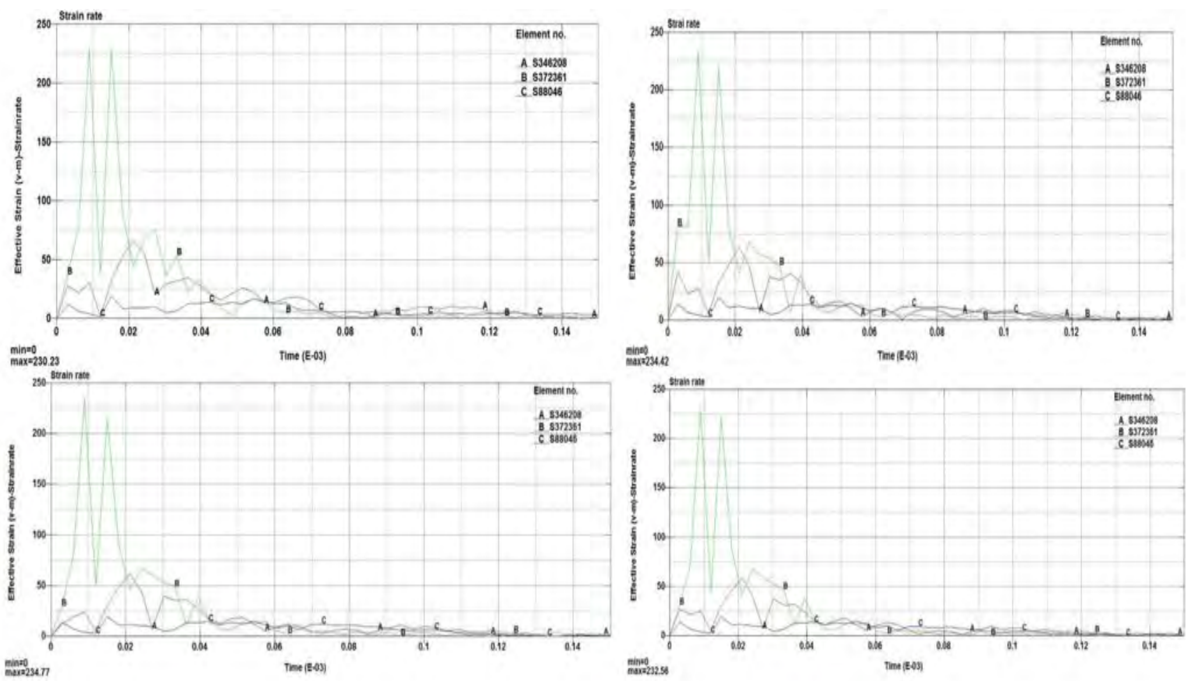

Figure 20: Strain rate comparison for Beta load case 1 - 10,000Hz .

Decay constant for load case 2-100,000Hz

Pressure

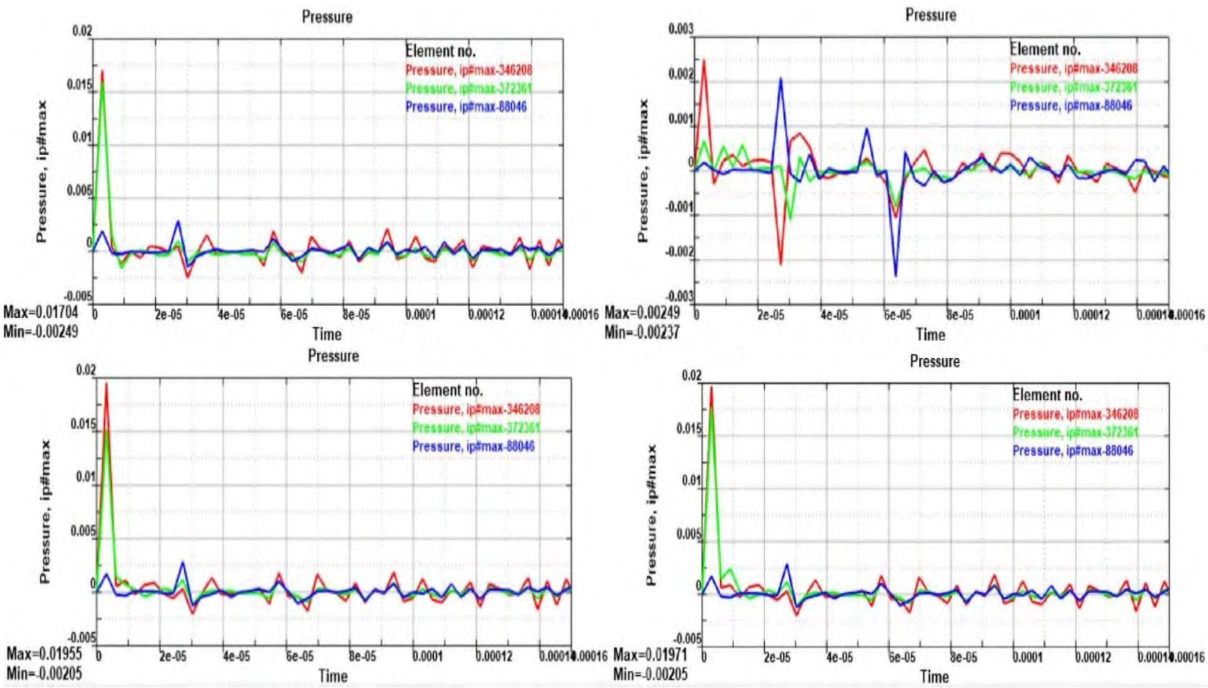

Figure 21: Pressure comparison for Beta load case 2 - 100,000Hz

Stress

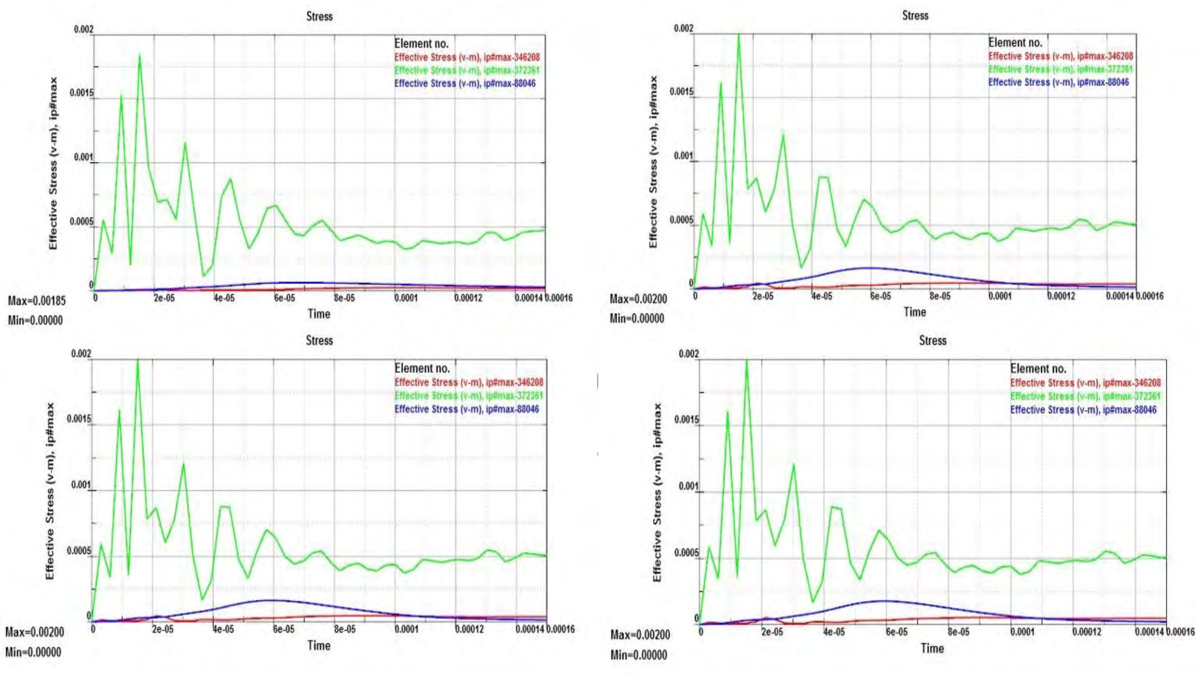

Figure 22: Stress comparison for Beta load case 2 - 100,000Hz .

Upper max Principal Strain

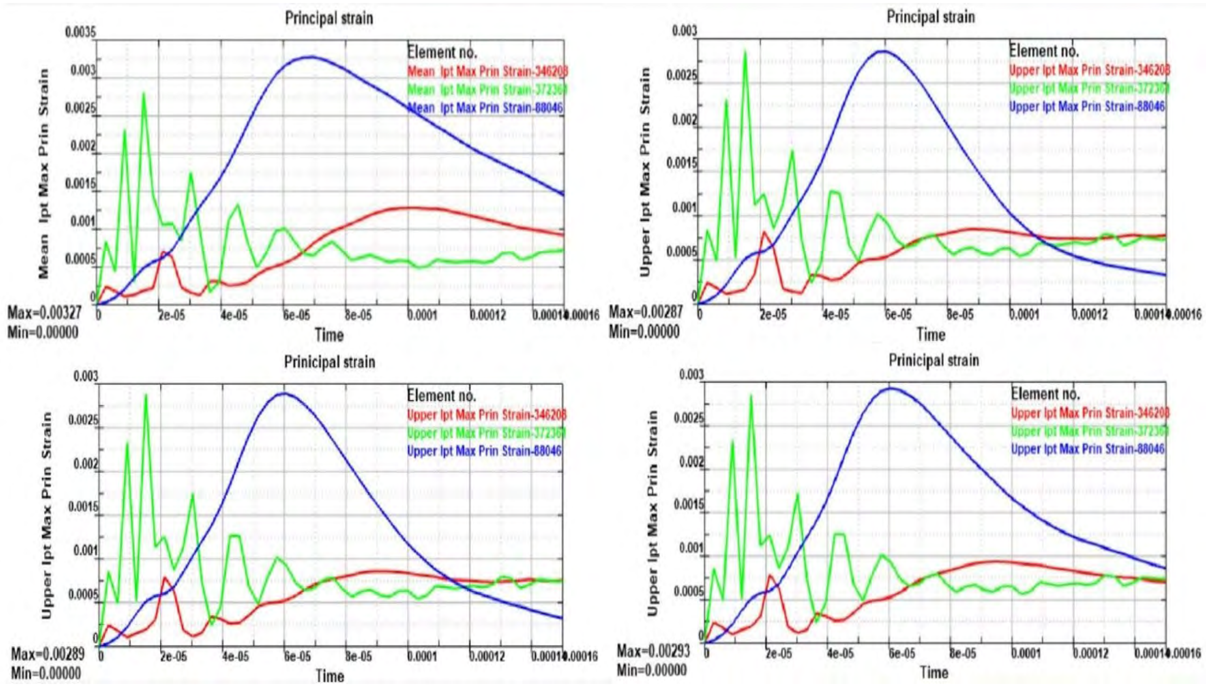

Figure 23: Upper max Principal Strain comparison for Beta load case 2 - 100,000Hz

Strain

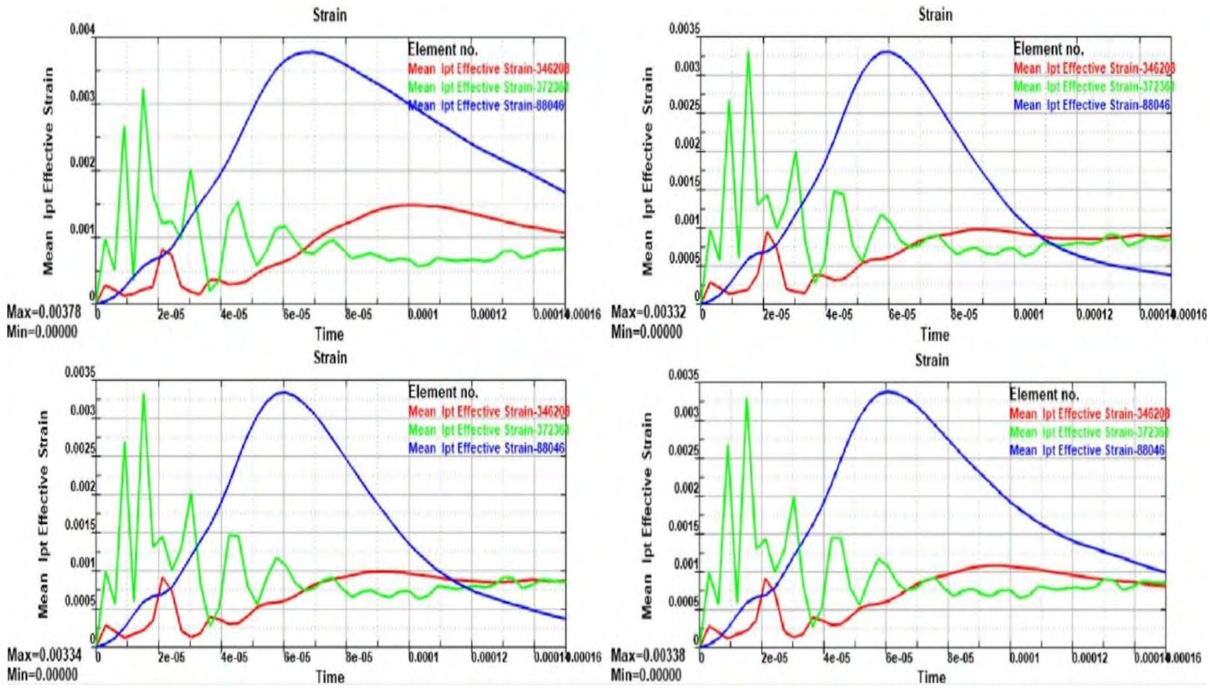

Figure 24: Strain comparison for Beta load case 2 - 100,000Hz .

Strain Rate

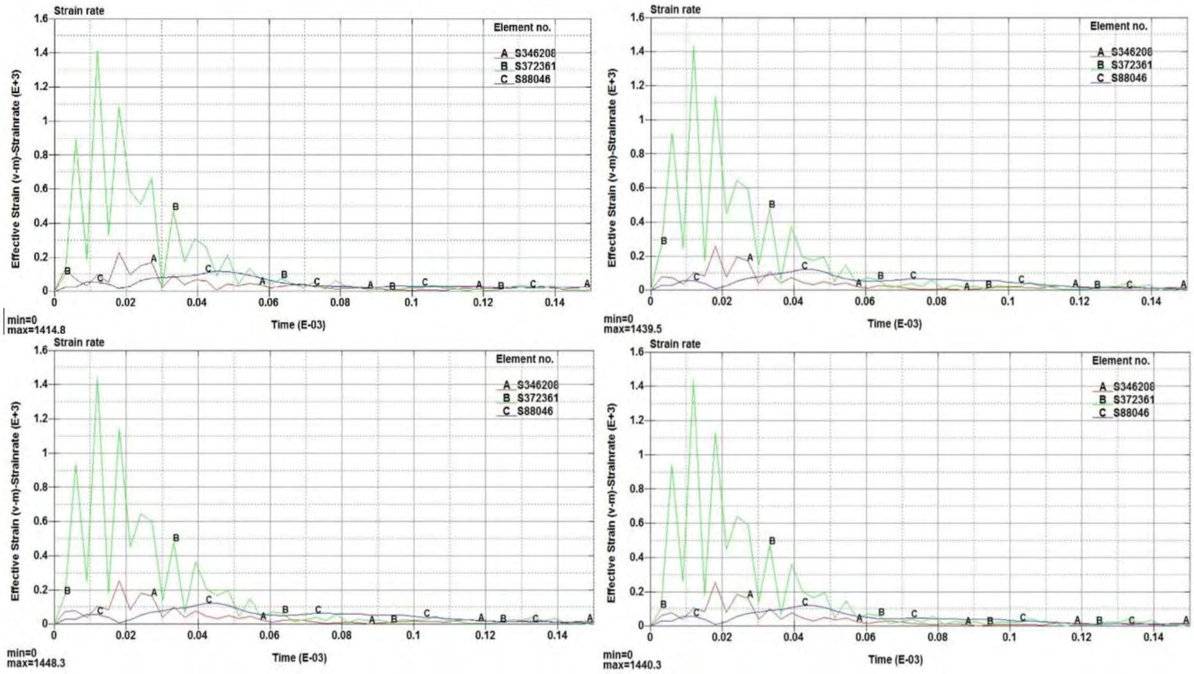

Figure 25: Strain rate comparison for Beta load case 2 - 100,000Hz .

8.2 Bulk modulus

Bulk modulus for load case 1 - 10,000Hz

Pressure

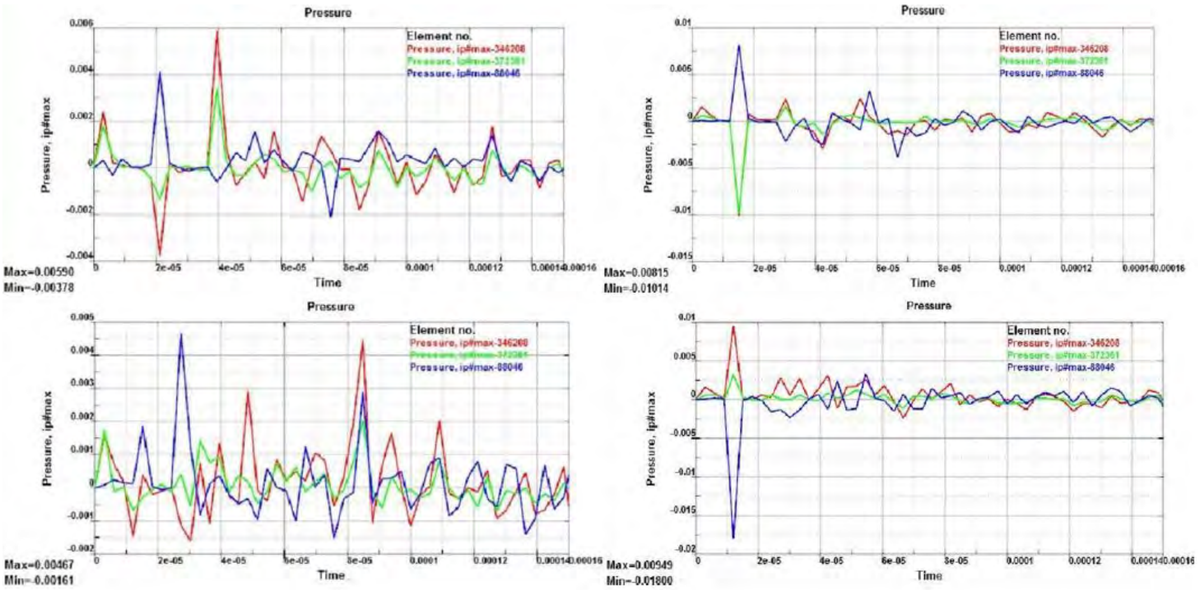

Figure 26: Pressure comparison for Bulk modulus load case 1 - 10,000Hz .

Stress

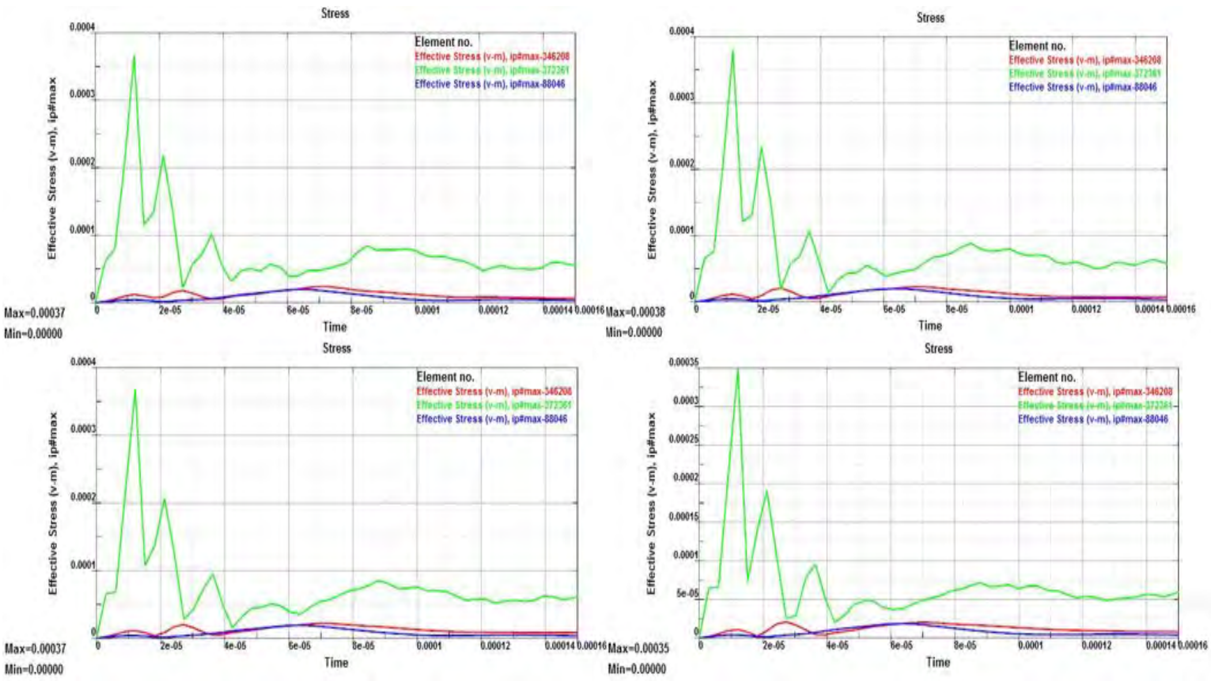

Figure 27: Stress comparison for Bulk modulus load case 1 - 10,000Hz .

Effective Strain

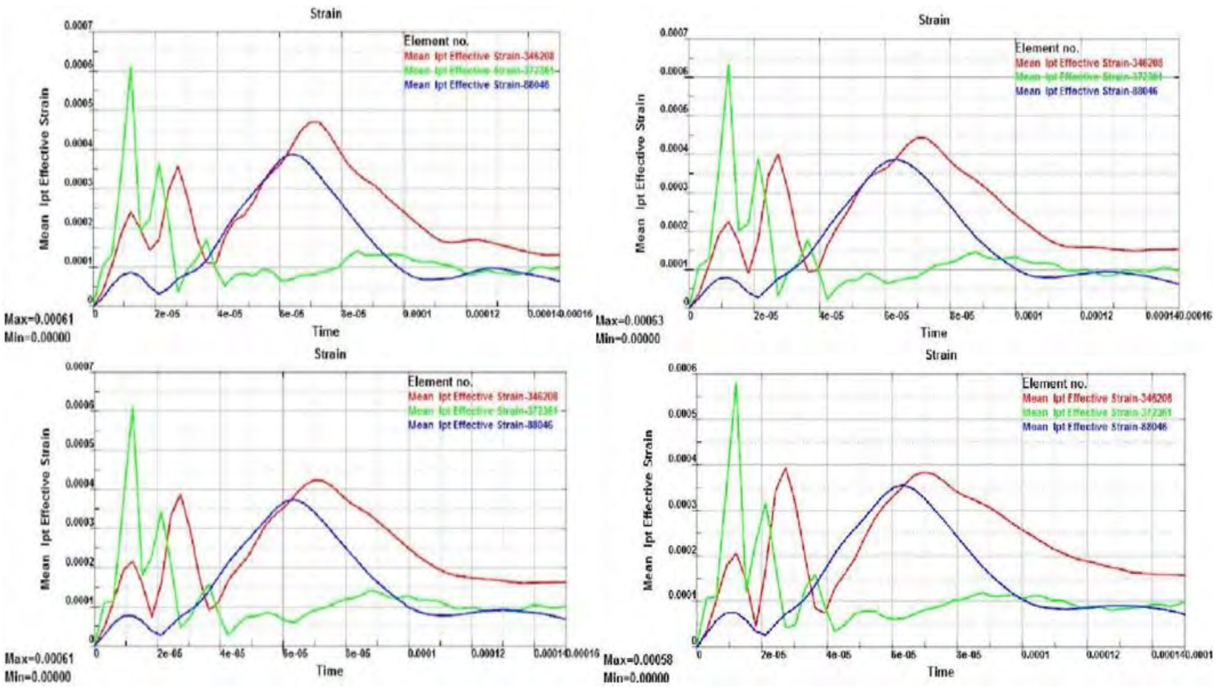

Figure 28: Effective Strain comparison for Bulk modulus load case 1 - 10,000Hz .

Upper max principal strain

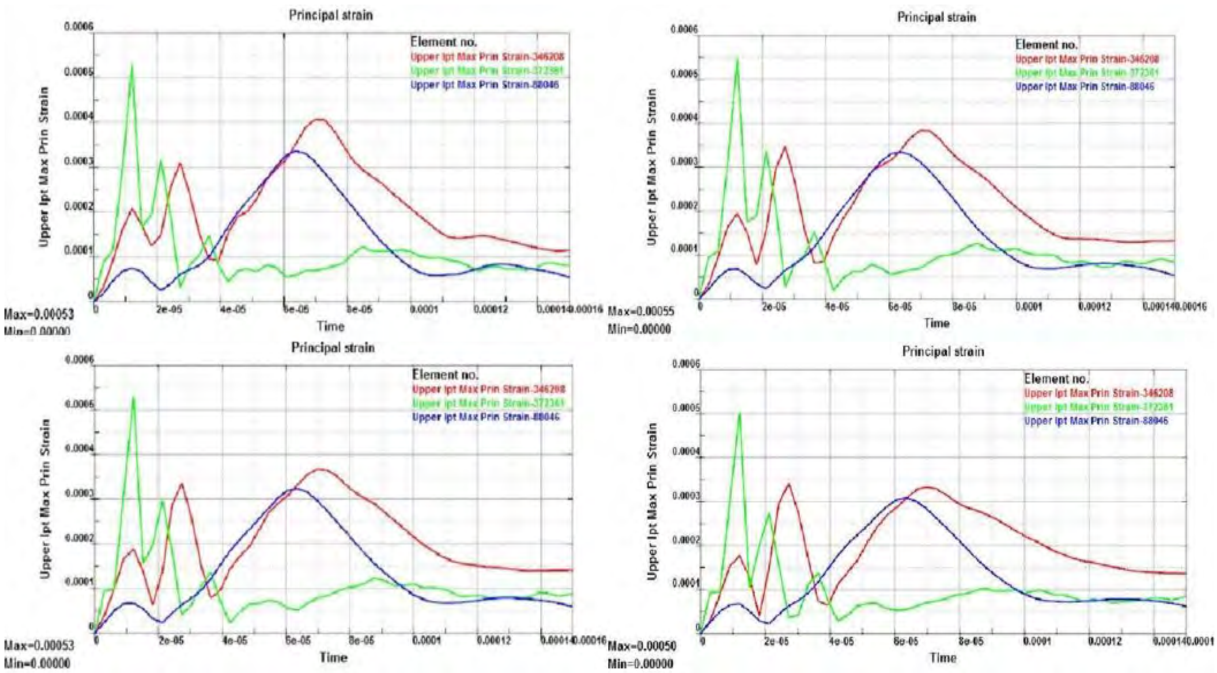

Figure 29: Upper max Principal Strain comparison for Bulk modulus load case 1 - 10,000Hz .

Strain rate

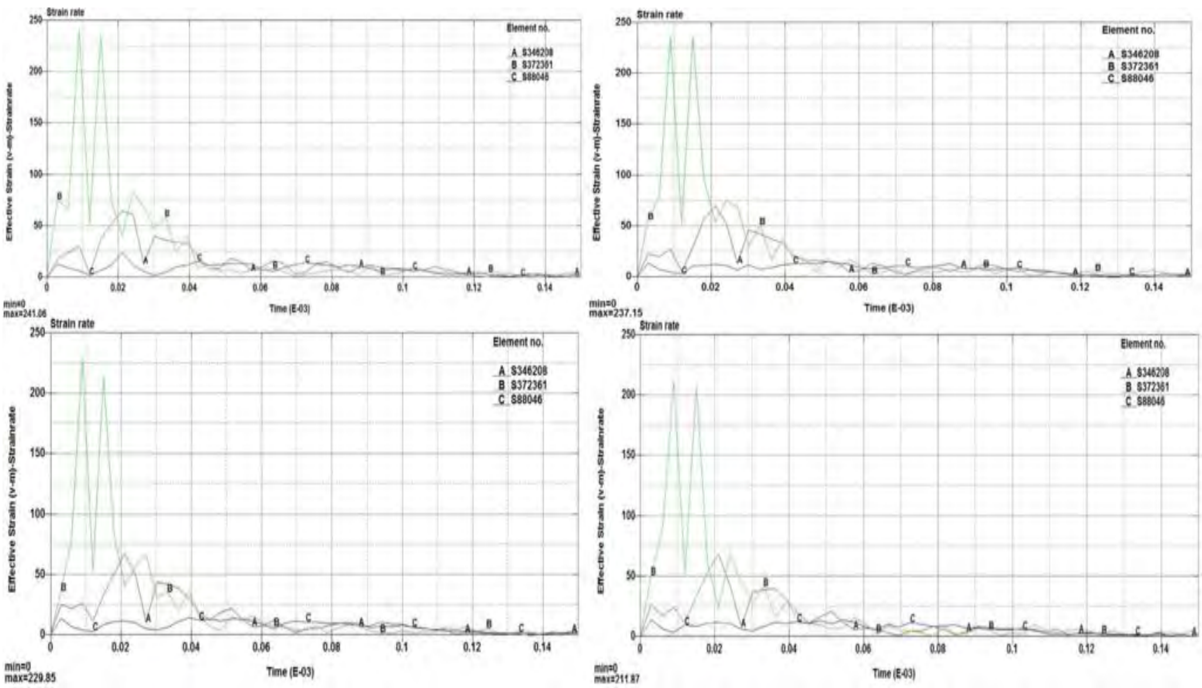

Figure 30: Strain rate comparison for Bulk modulus load case 1- 10,000Hz.

Bulk modulus for load case 2 -100,000Hz

Pressure

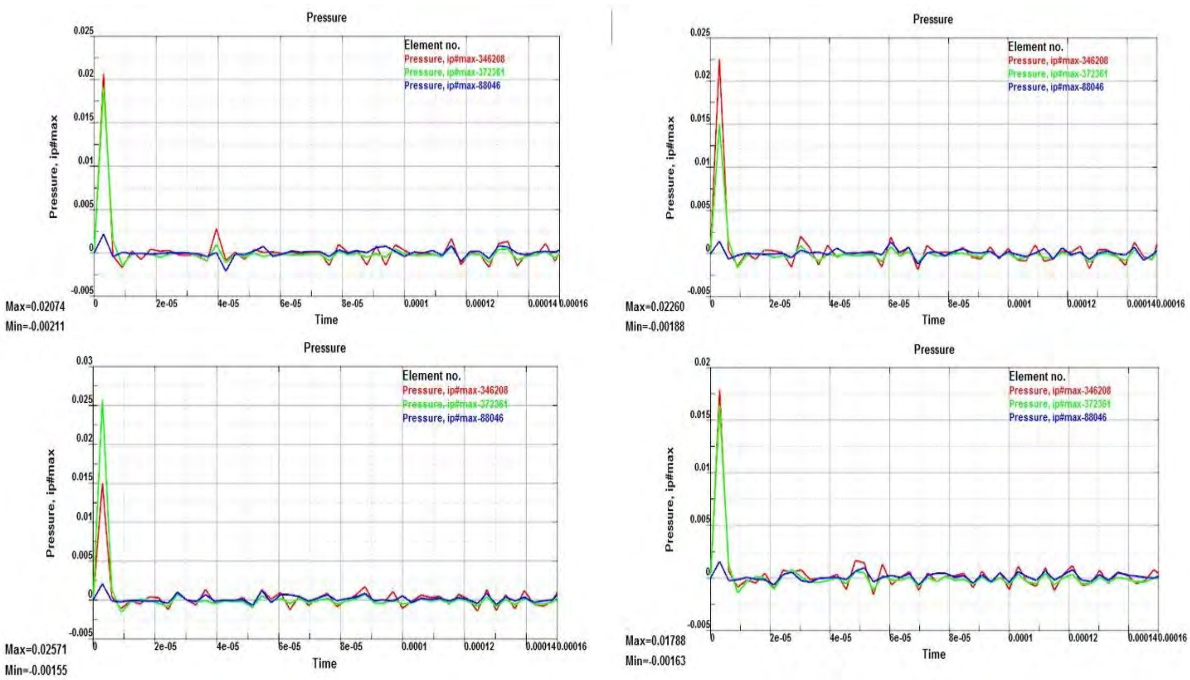

Figure 31: Pressure comparison for Bulk modulus load case 2- 100,000Hz .

Stress

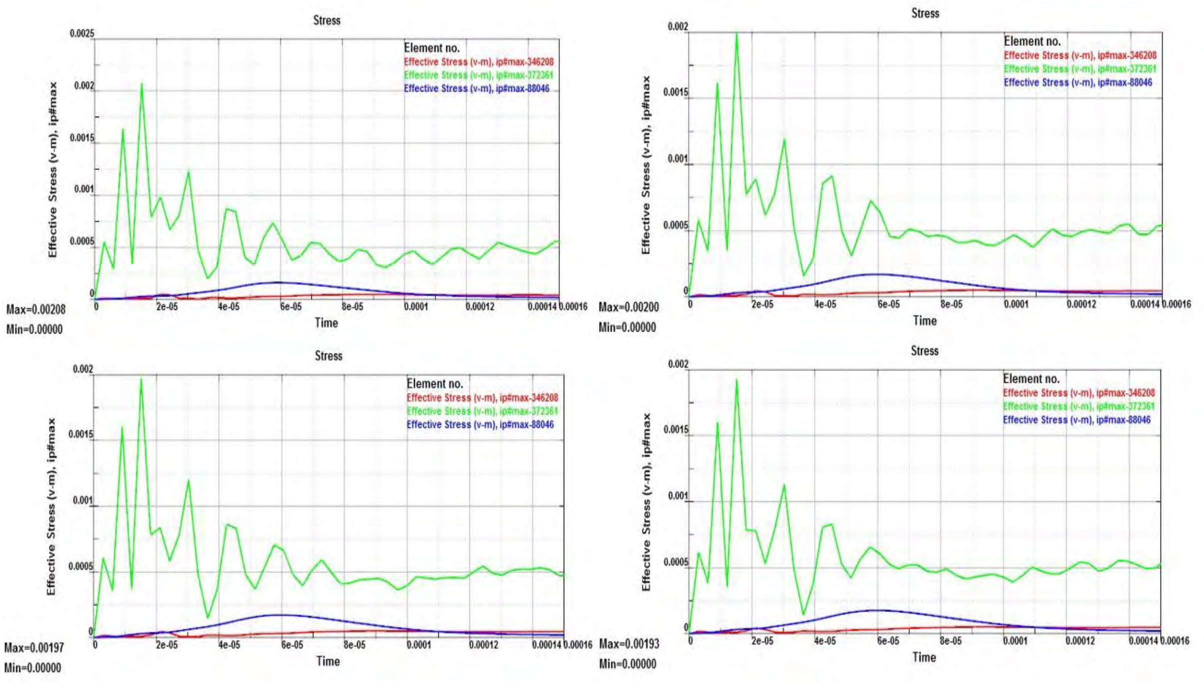

Figure 32: Stress comparison for Bulk modulus load case 2 - 100,000Hz .

Effective Strain

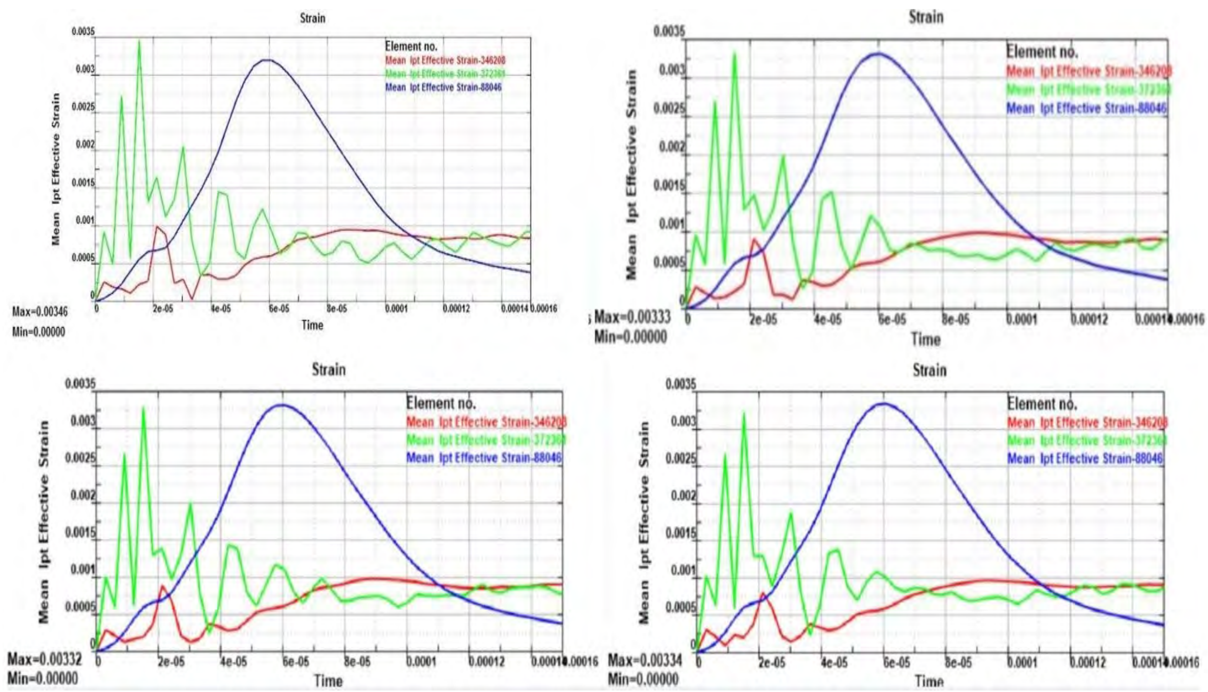

Figure 33: Strain comparison for Bulk modulus load case 2 - 100,000Hz .

Upper max principal strain

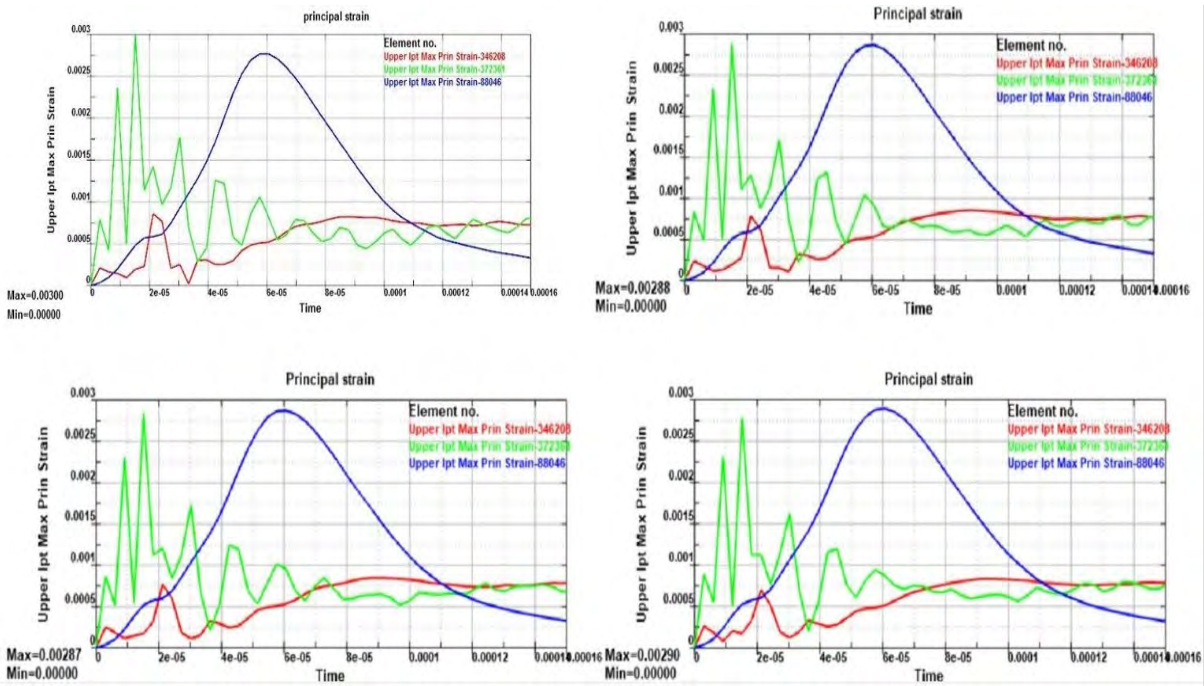

Figure 34: Upper max Principal Strain comparison for Bulk modulus load case 2 - 100,000Hz .

Strain rate

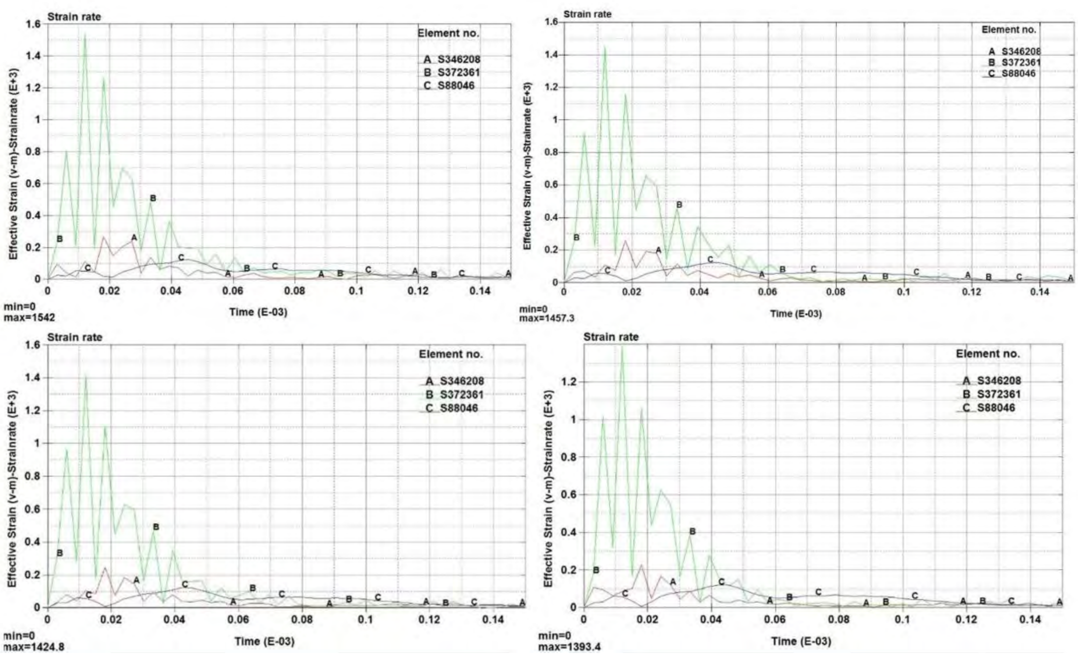

Figure 35: Strain rate comparison for Bulk modulus load case 2 - 100,000Hz .

8.3 Shear Modulus load case 1- 10,000Hz

Pressure

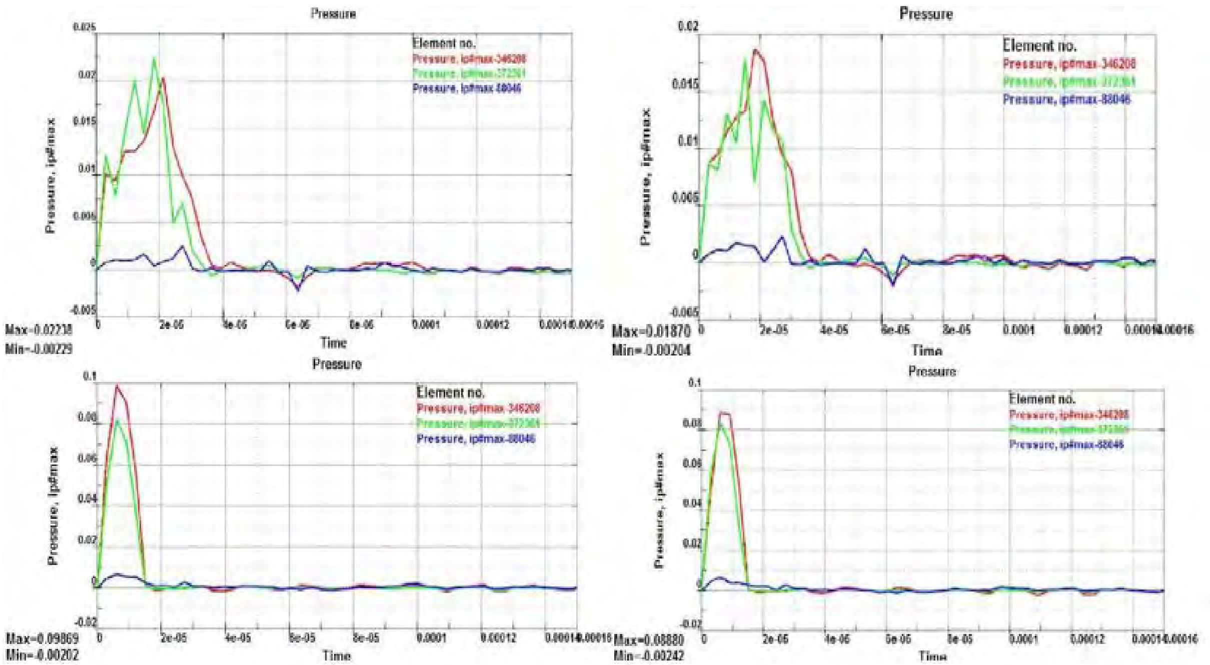

Figure 36: Pressure comparison for shear modules 1 to 4 for load case 1 - 10,000Hz

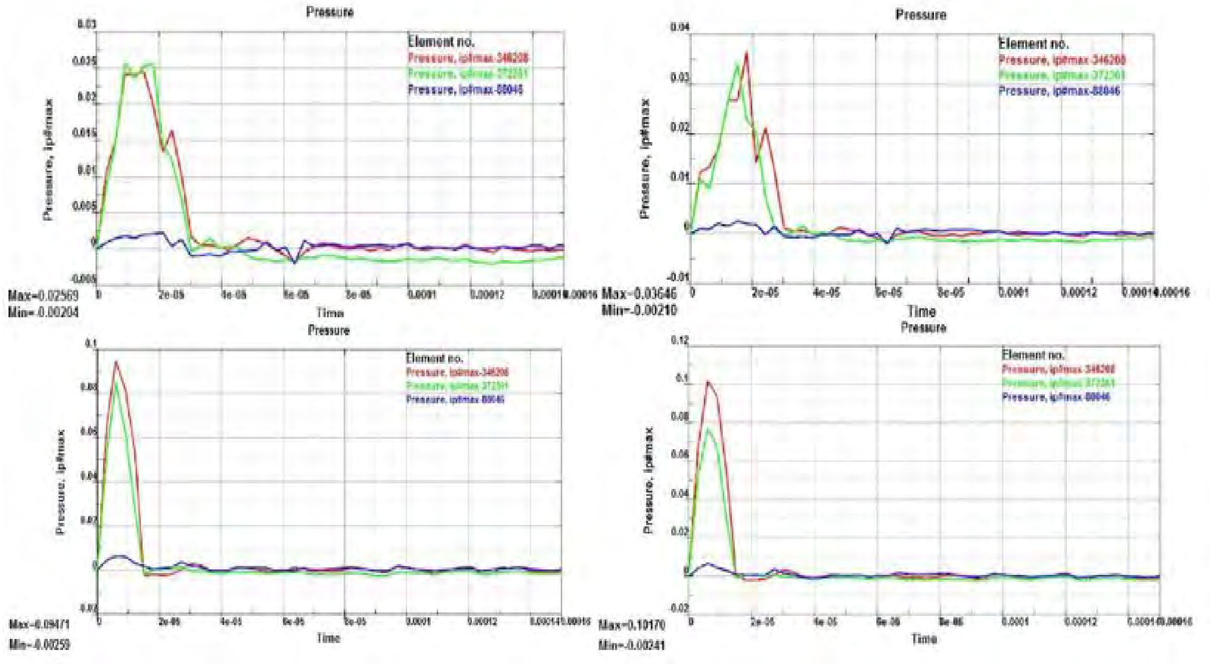

Figure 37: Pressure comparison for shear modules 5 to 8 for load case 1 - 10,000Hz

Stress

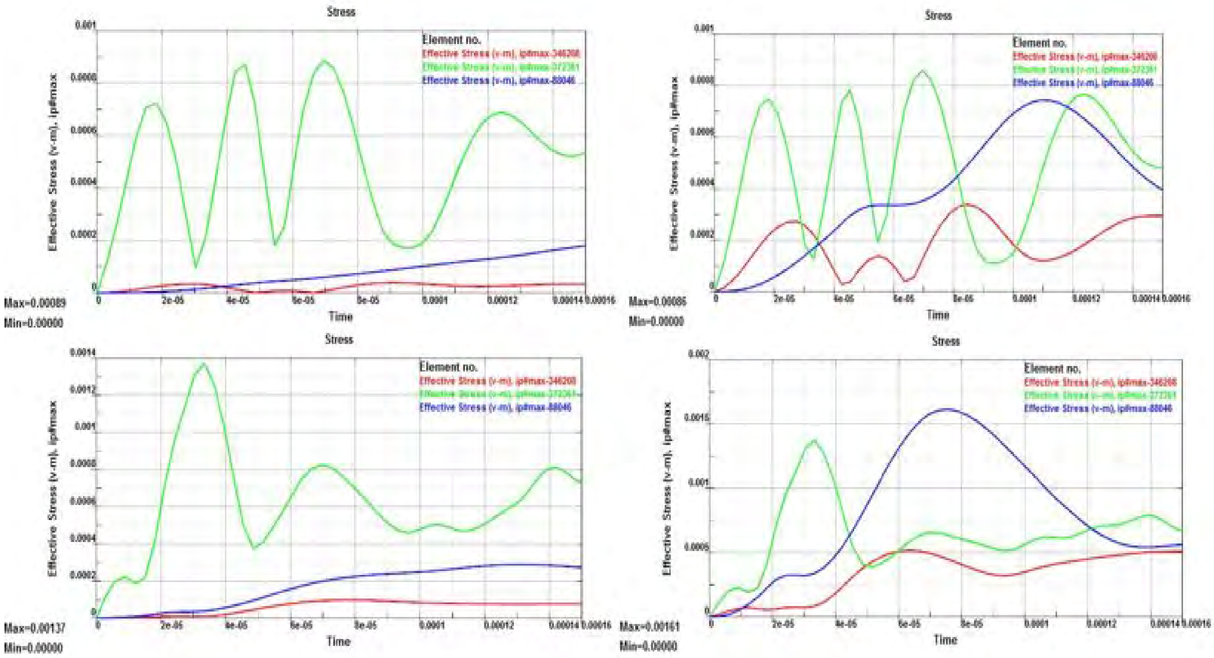

Figure 38: Stress comparison for shear modules 1 to 4 for load case 1 - 10,000Hz

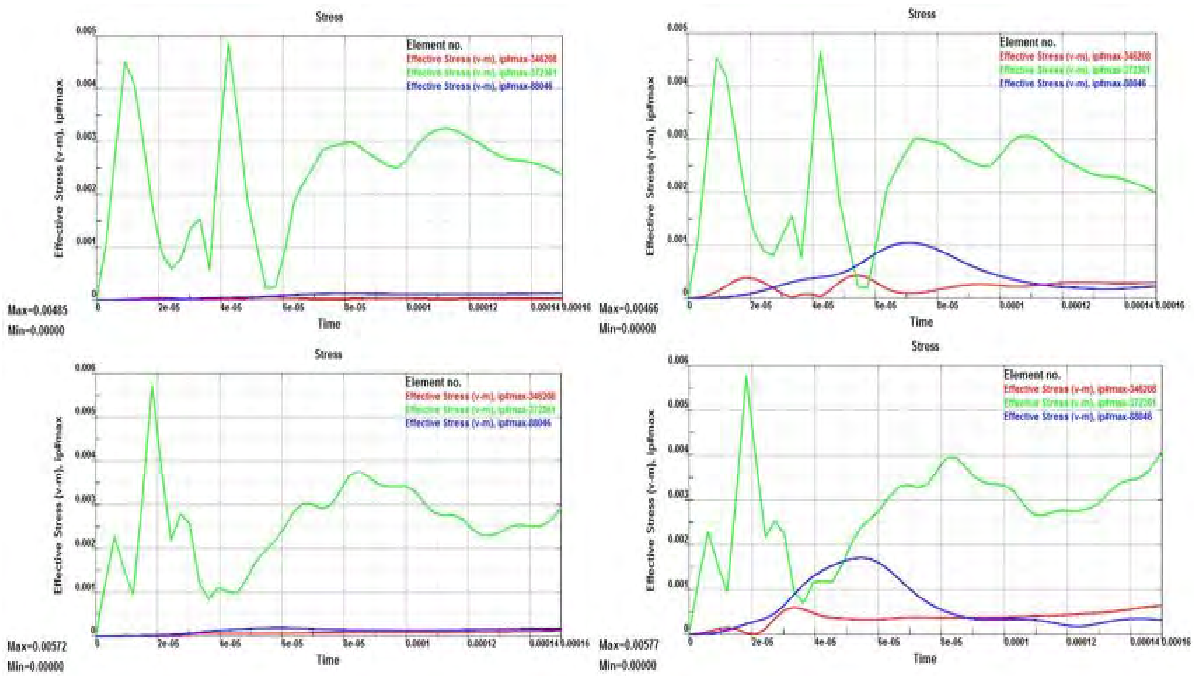

Figure 39: Stress comparison for shear modules 5 to 8 for load case 1 - 10,000Hz

Upper max Principal Strain

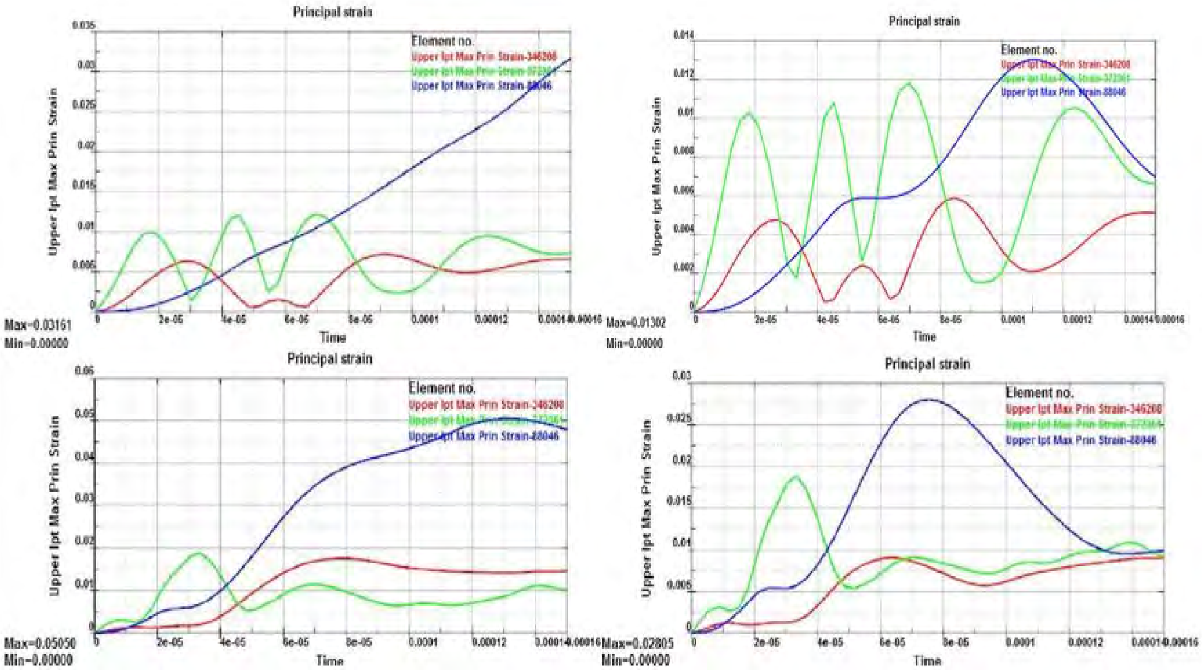

Figure 40: Principal Strain comparison for shear modules 1 to 4 for load case 1 - 10,000Hz

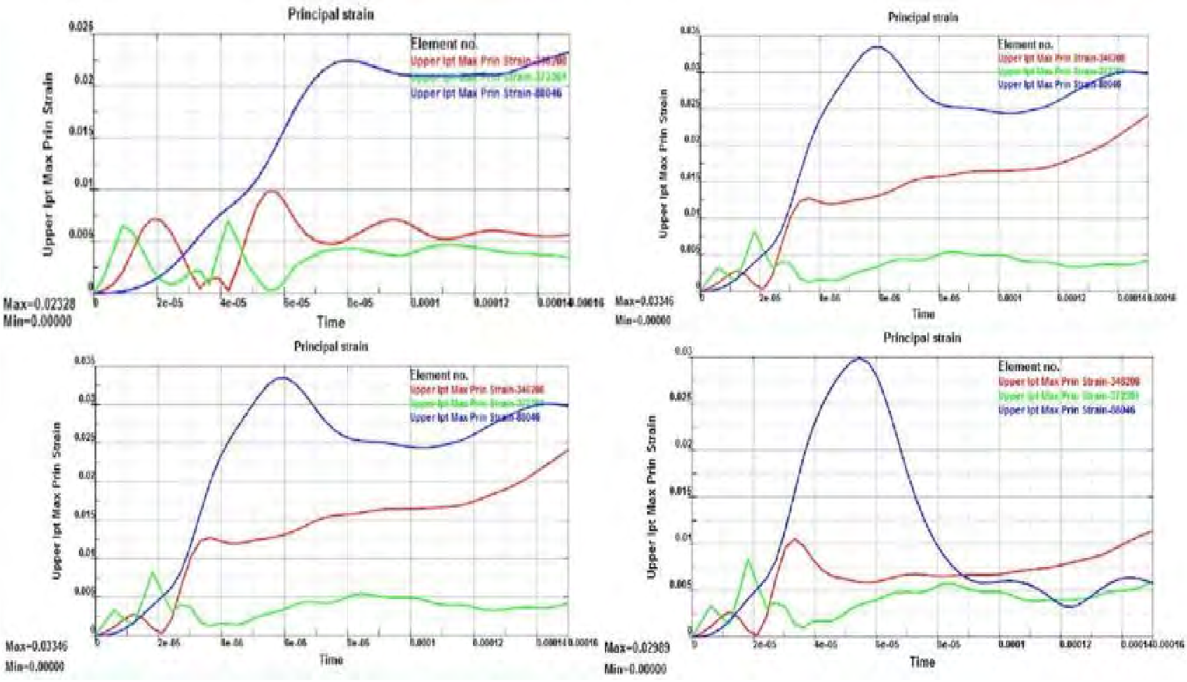

Figure 41: Principal Strain comparison for shear modules 5 to 8 for load case 1 - 10,000Hz

Strain

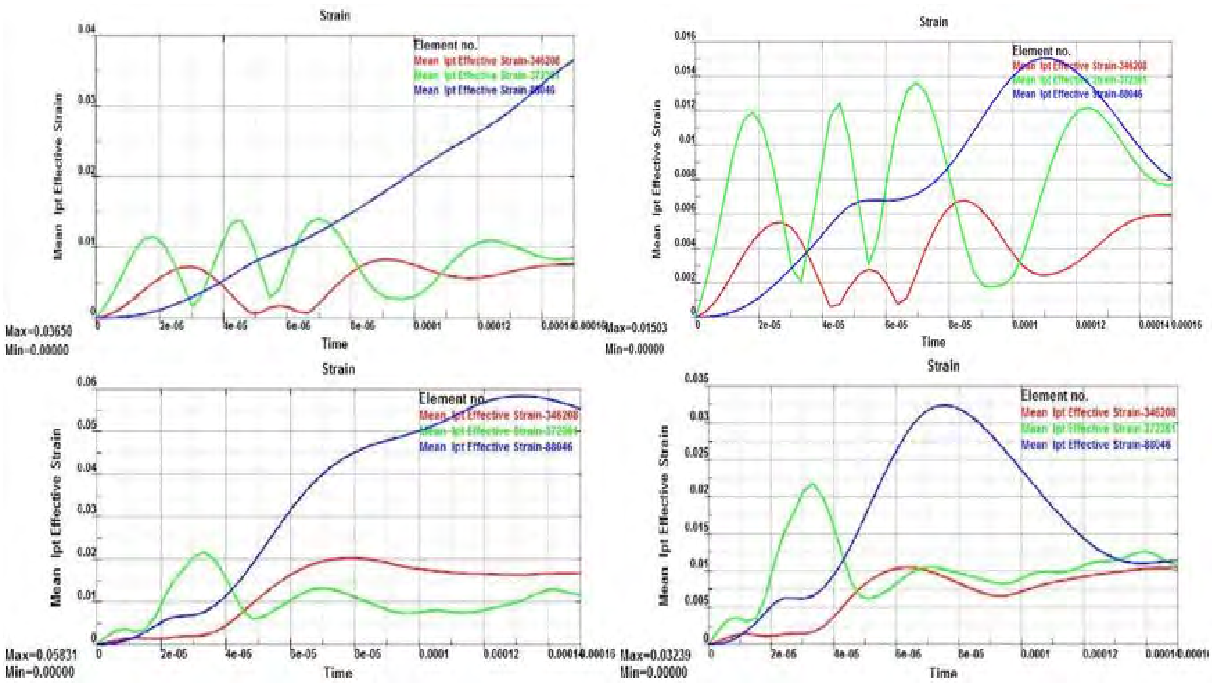

Figure 42: Principal Strain comparison for shear modules 1 to 4 for load case 1 - 10,000Hz

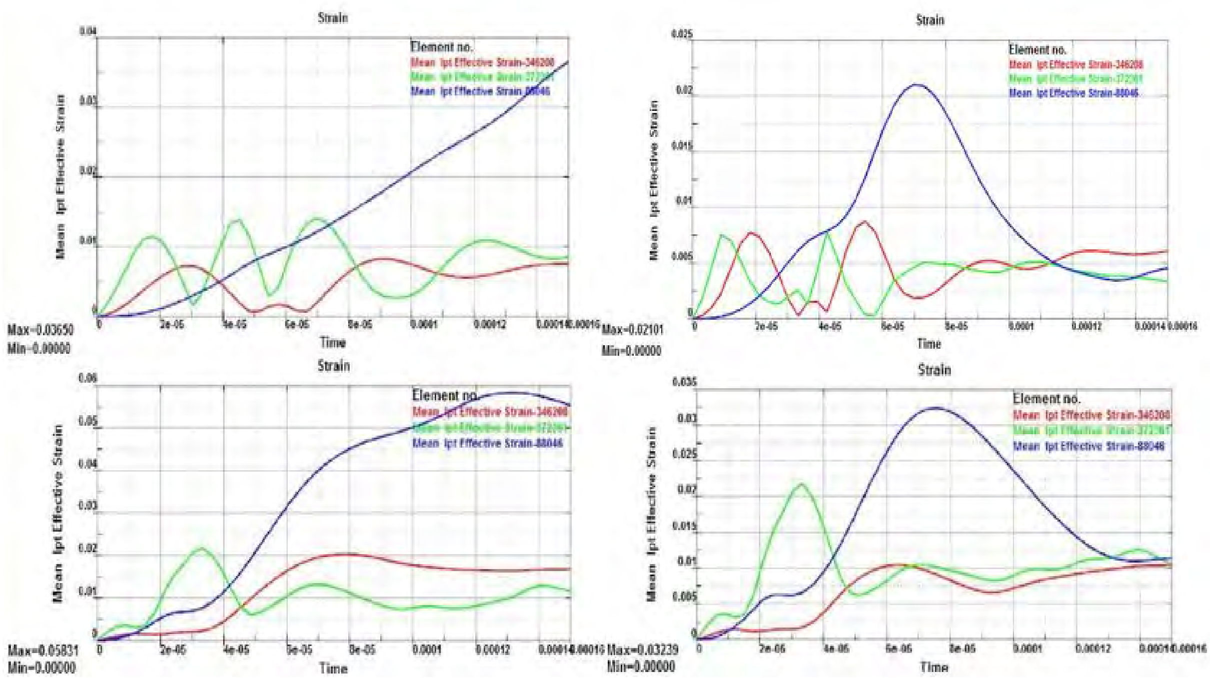

Figure 43: Principal Strain comparison for shear modules 5 to 8 for load case 1 - 10,000Hz

Strain Rate

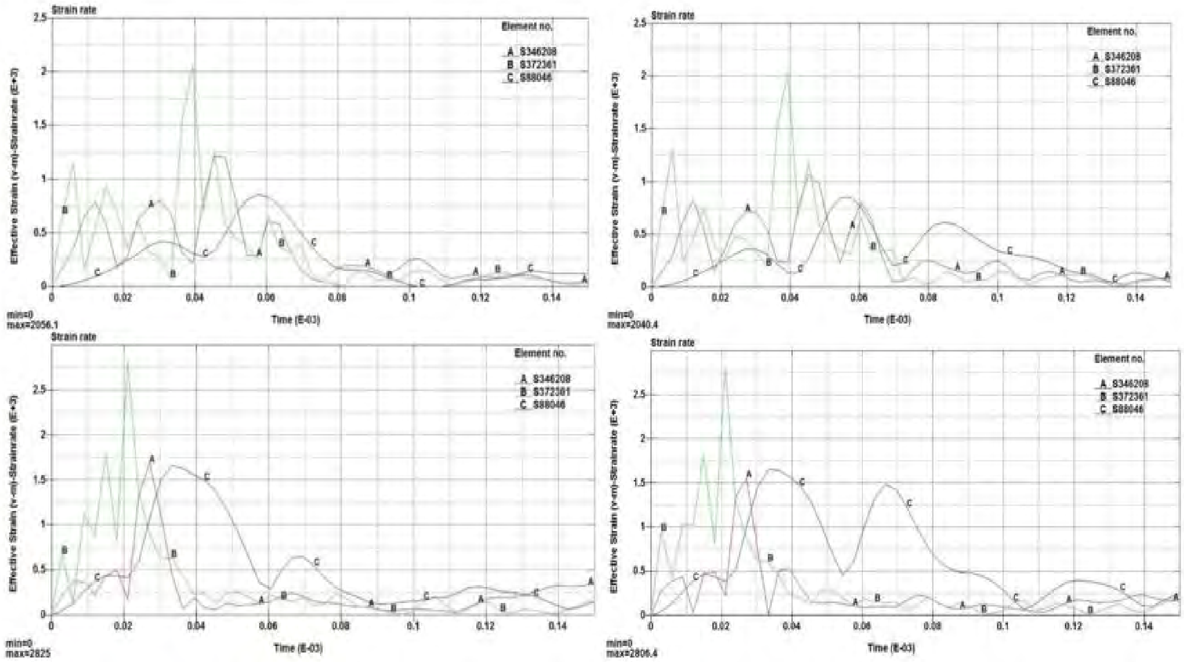

Figure 44: Strain Rate comparison for shear modules 1 to 4 for load case 1 - 10,000Hz

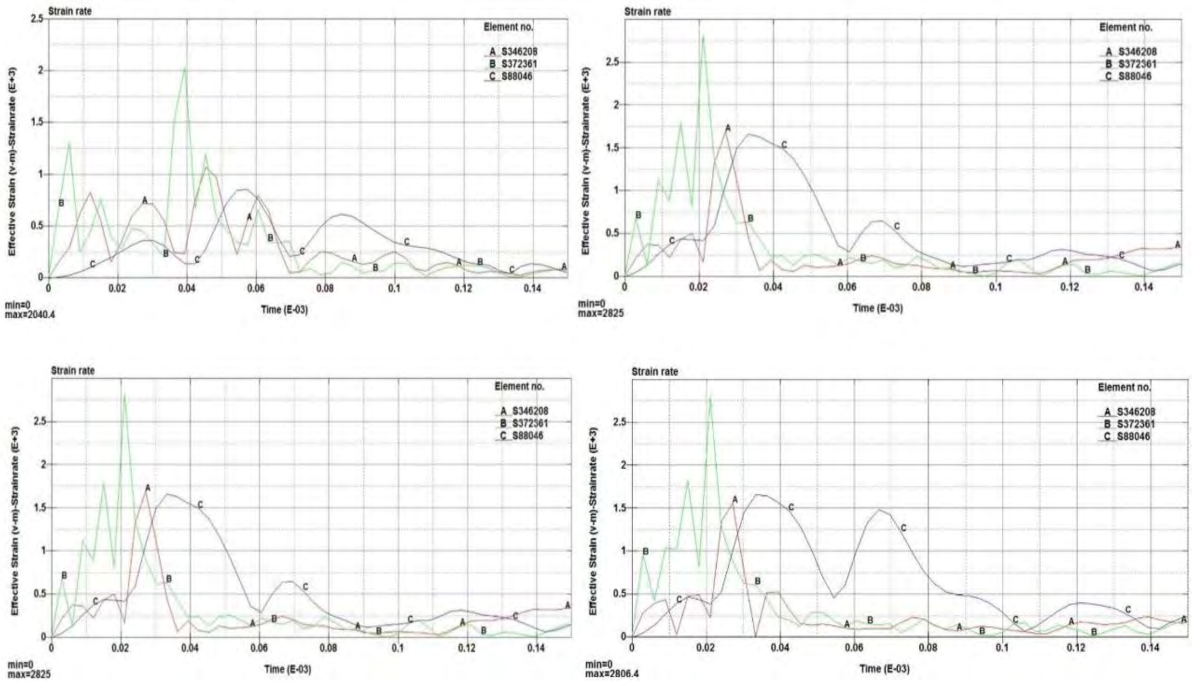

Figure 45: Strain Rate comparison for shear modules 5 to 8 for load case 1 - 10,000Hz

shear modules for load case 2 - 100,000Hz

Pressure

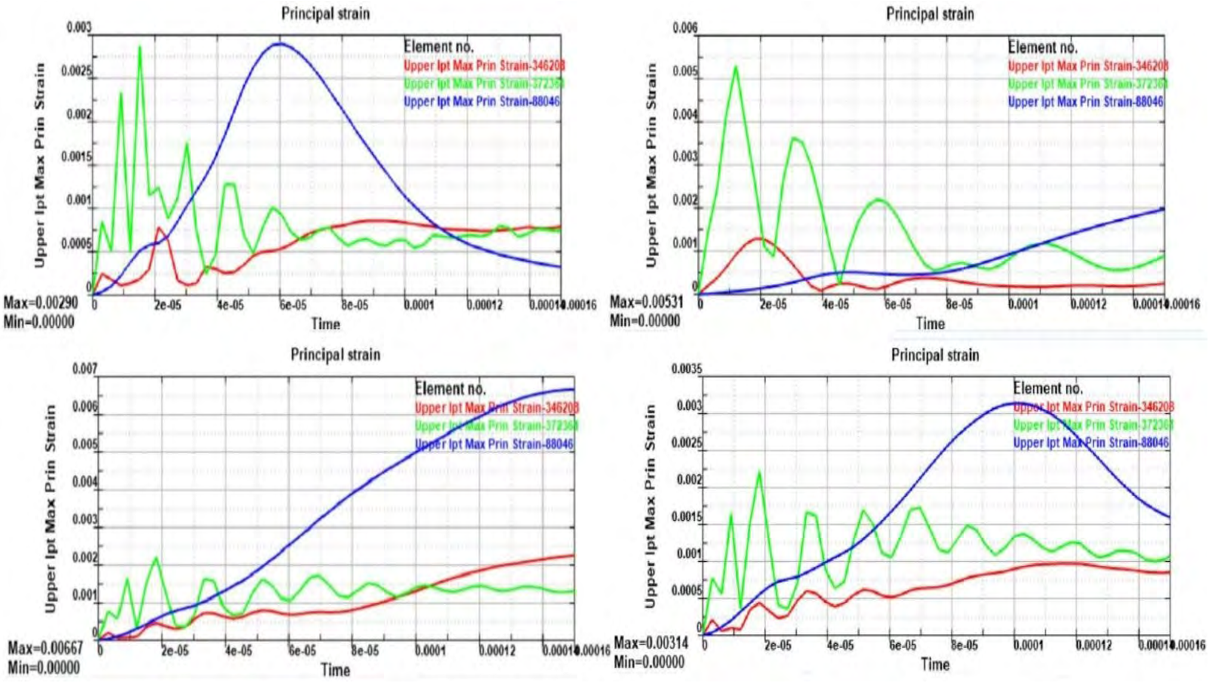

Figure 46: Pressure comparison for shear modules 1 to 4 for load case 2 - 100,000Hz

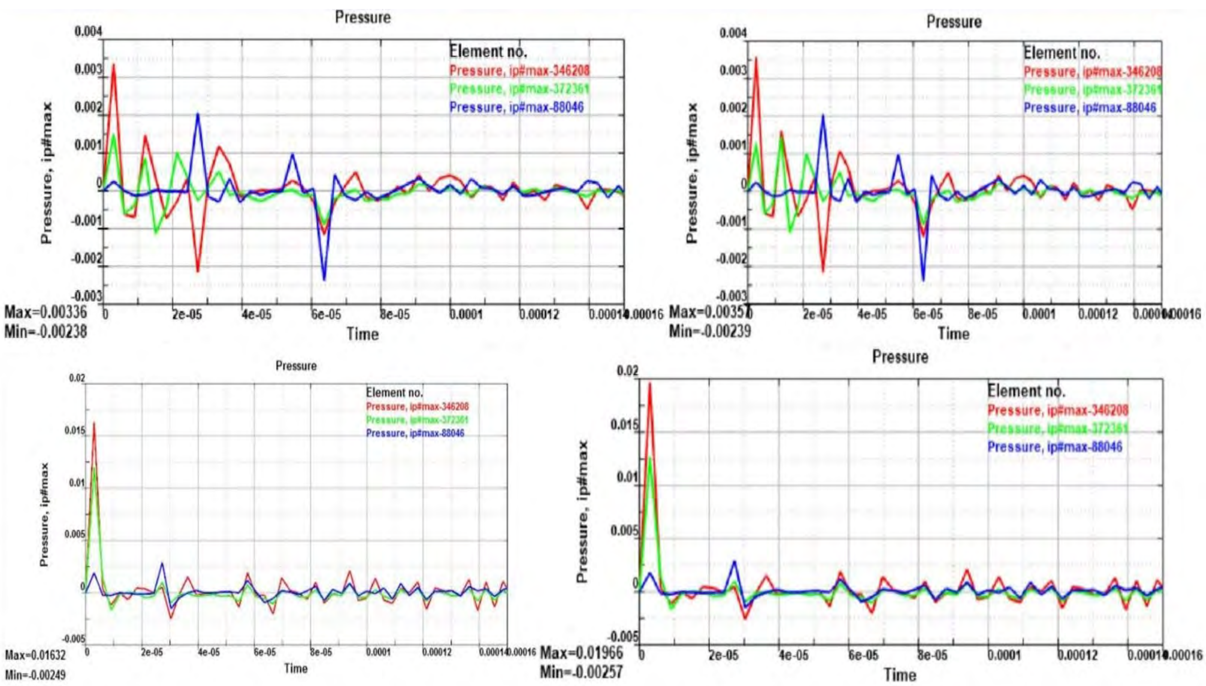

Figure 47: Pressure comparison for shear modules 5 to 8 for load case 2 - 100,000Hz

Stress

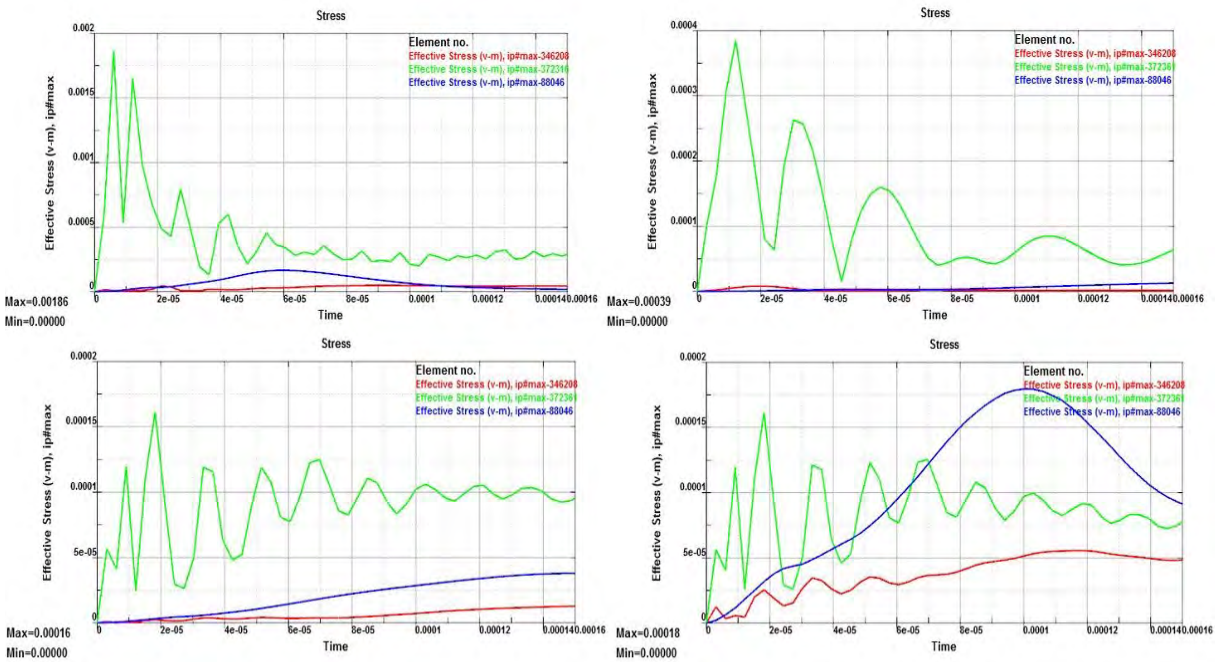

Figure 48: Stress comparison for shear modules 1 to 4 for load case 2 - 100,000Hz

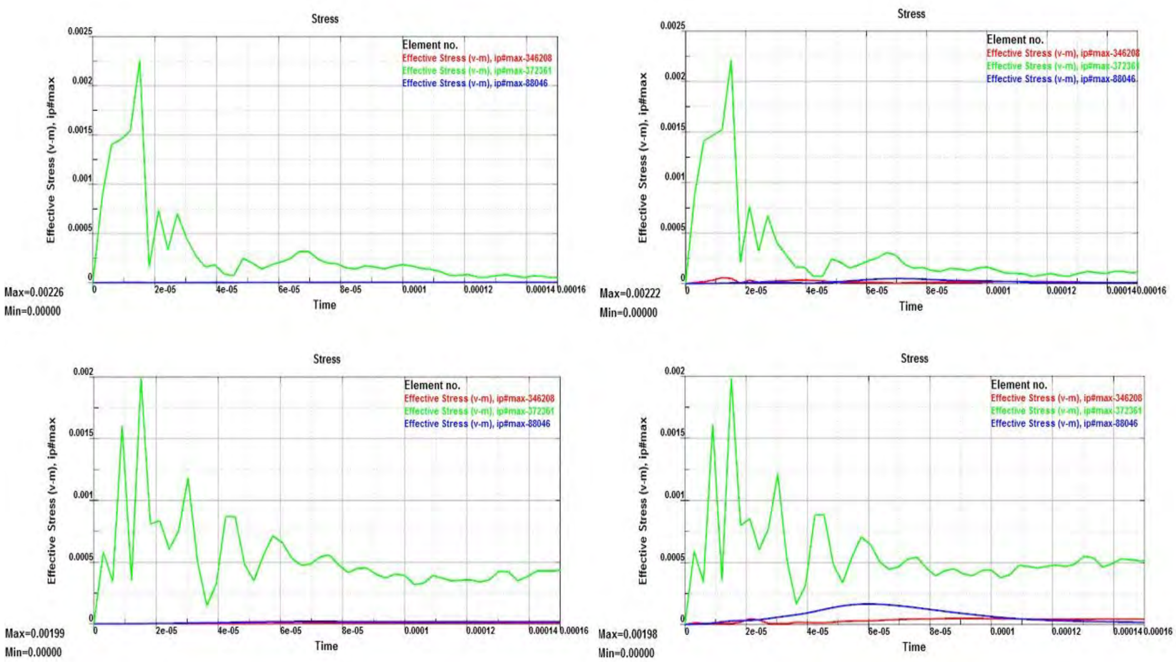

Figure 49: Stress comparison for shear modules 5 to 8 for load case 2 - 100,000Hz

Upper max Principal Strain

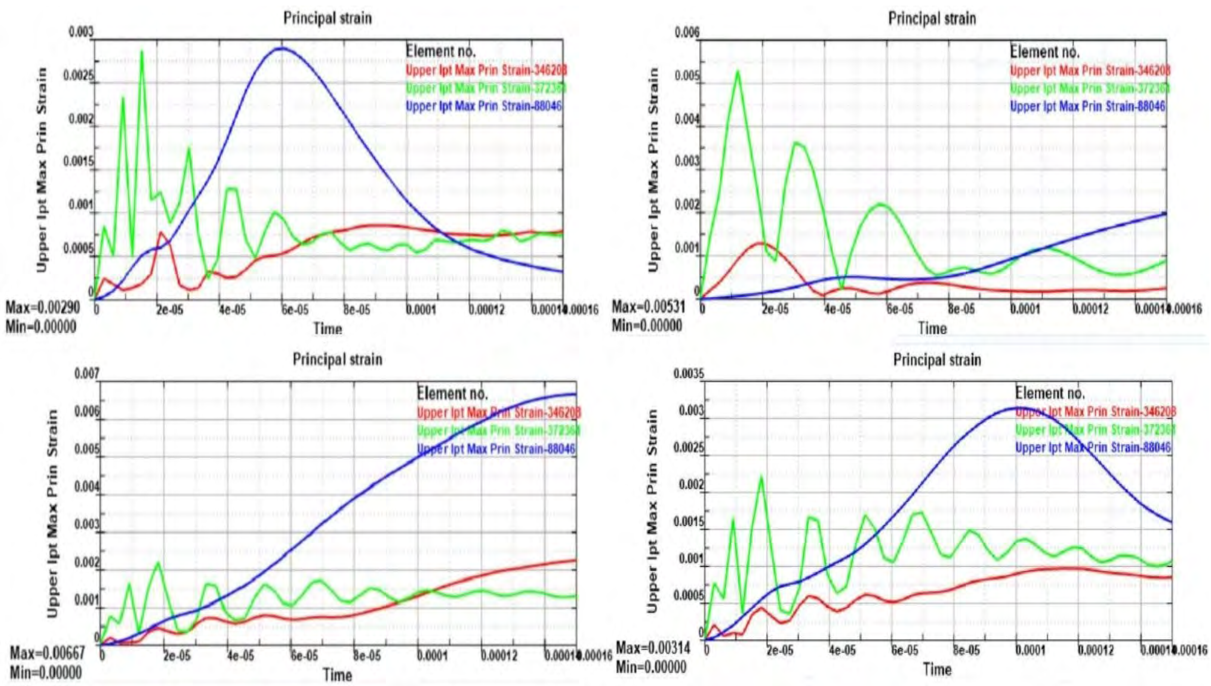

Figure 50: Principal Strain comparison for shear modules 1 to 4 for load case 2 - 100,000Hz

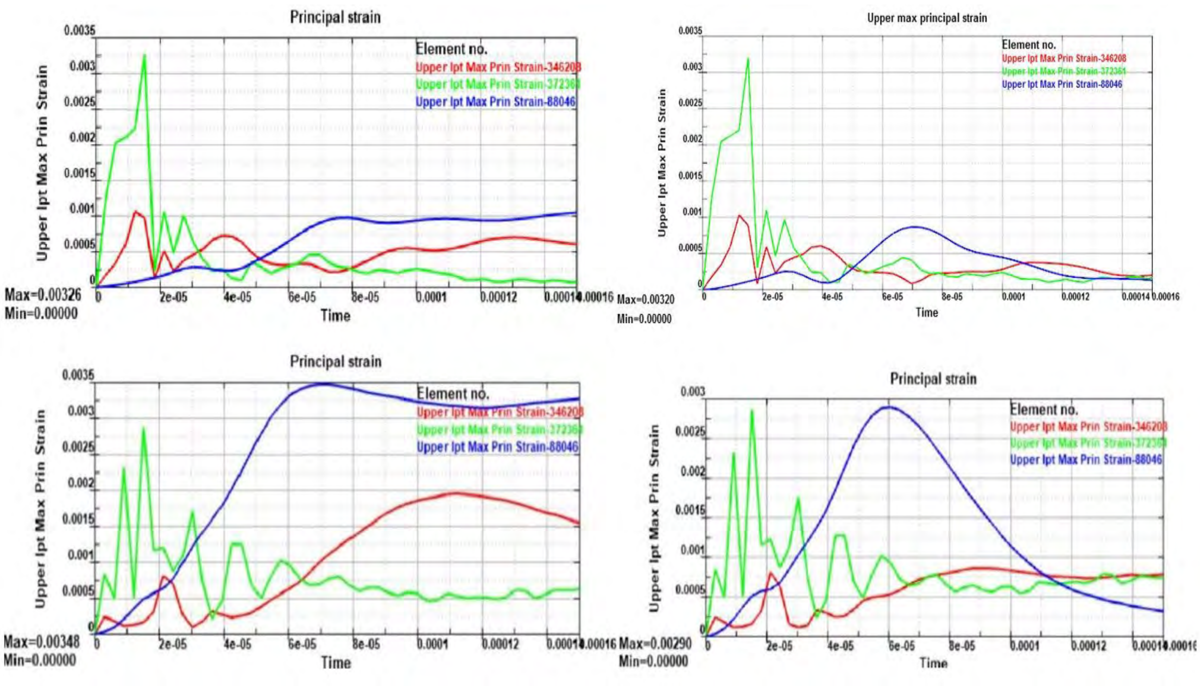

Figure 51: Principal Strain comparison for shear modules 5 to 8 for load case 2 - 100,000Hz

Strain

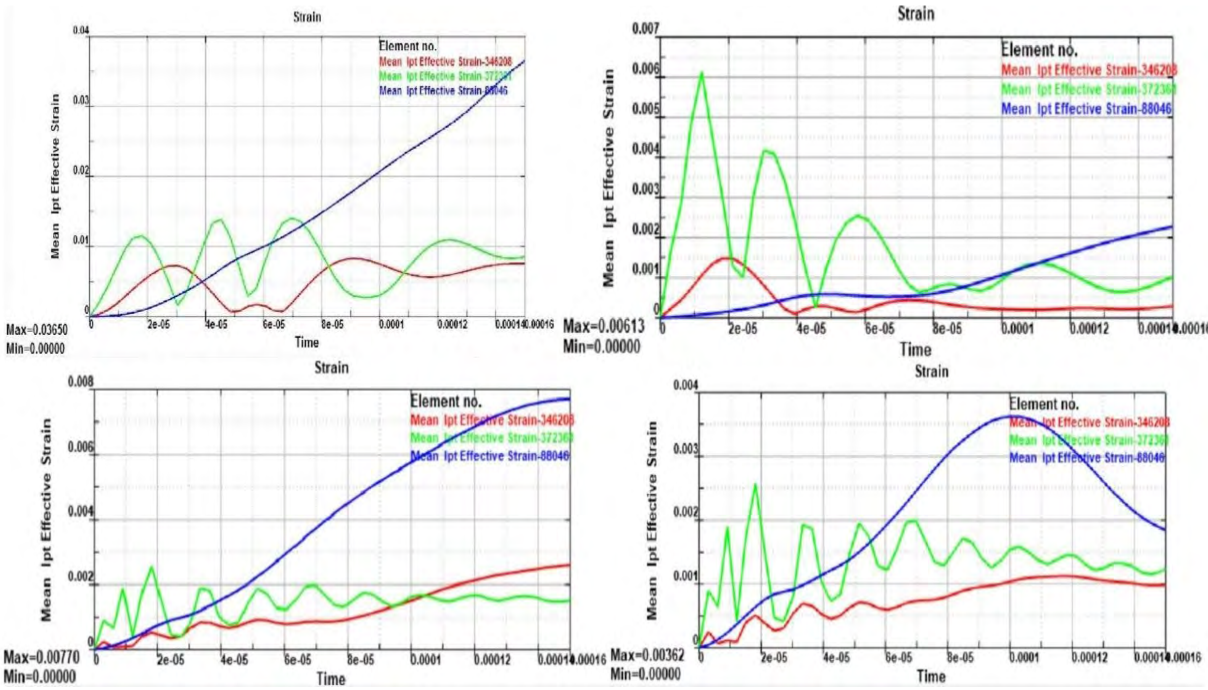

Figure 52: Effective Strain comparison for shear modules 1 to 4 for load case 2 - 100,000Hz

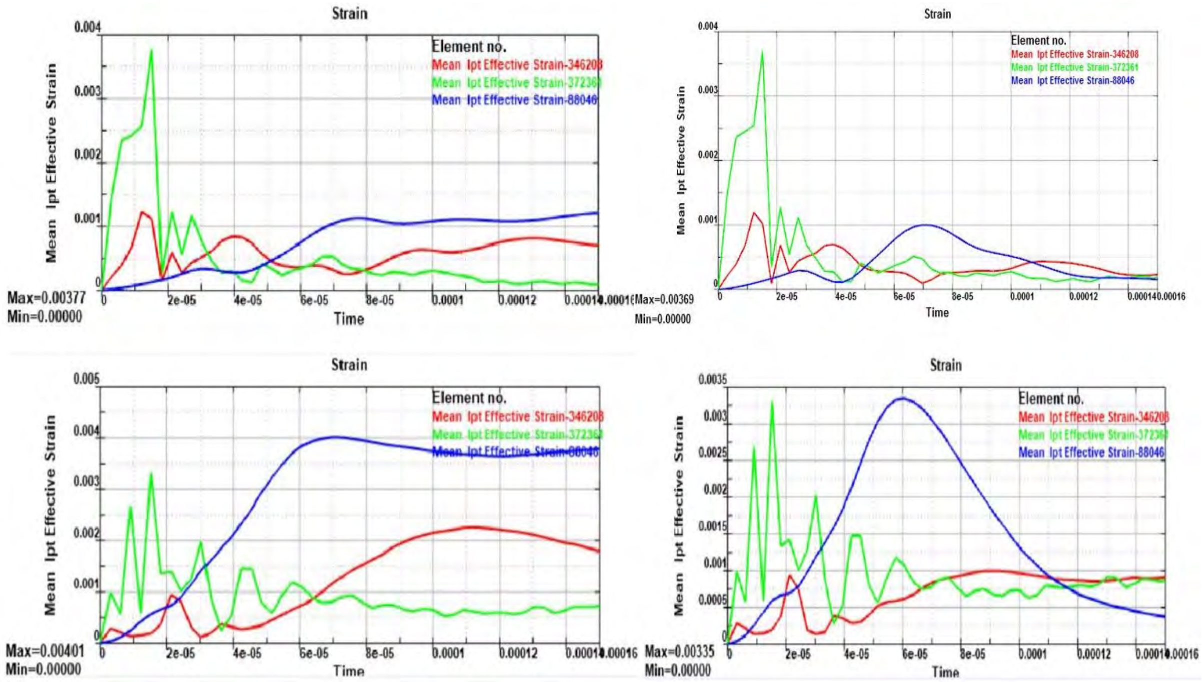

Figure 53: Effective Strain comparison for shear modules 5 to 8 for load case 2 - 100,000Hz

Strain Rate

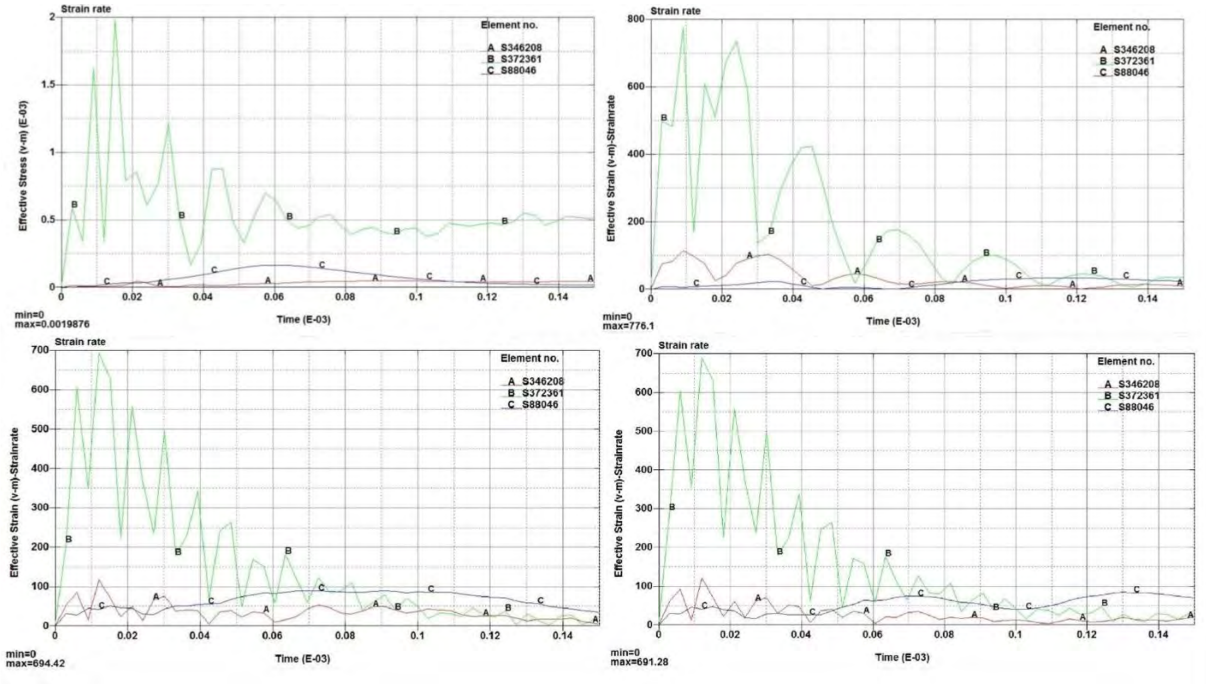

Figure 54: Strain Rate comparison for shear modules 1 to 4 for load case 2 - 100,000Hz

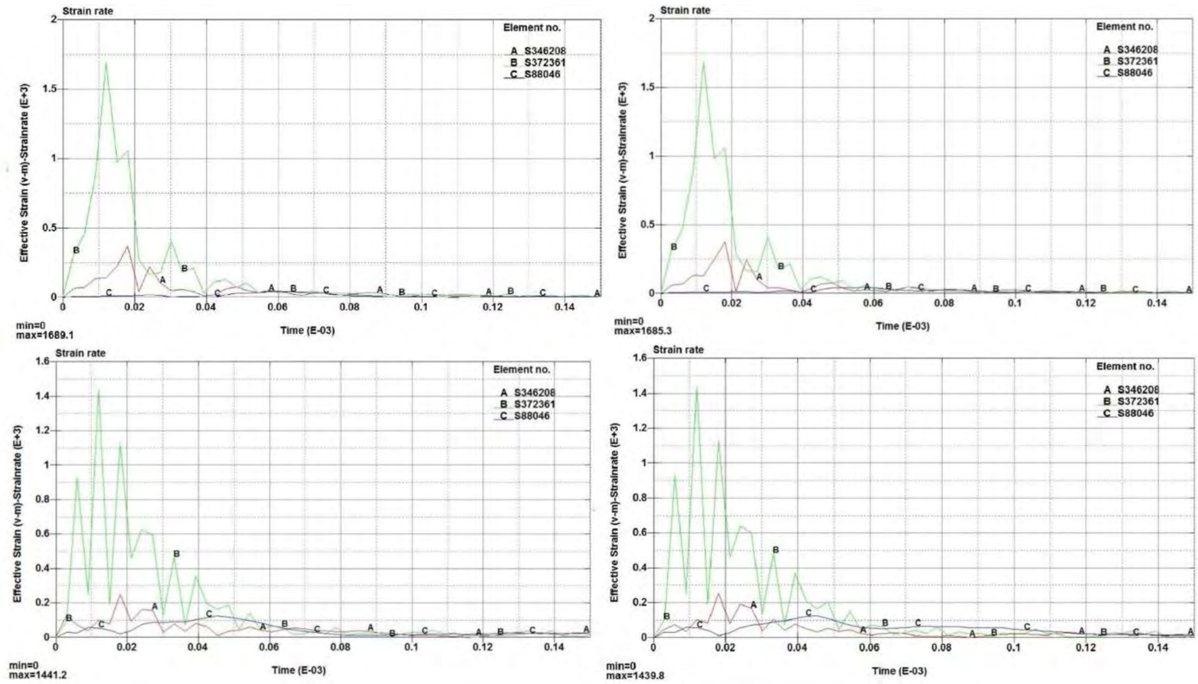

Figure 55: Strain Rate comparison for shear modules 5 to 8 for load case 2 - 100,000Hz